---

**Article:**
Roychoudhry, S. orcid.org/0000-0002-9736-0269 and Kepinski, S. orcid.org/0000-0001-9819-5034 (2023) PIN phospho-regulation drives gravity-dependent non-vertical growth in Arabidopsis roots. Nature Plants, 9. pp. 1383-1384. ISSN 2055-026X

https://doi.org/10.1038/s41477-023-01479-w

---

1

| Figure or Table #<br>Please group Extended Data items by type, in sequential order. Total number of items (Figs. + Tables) must not exceed 10. | Figure/Table title<br>One sentence only | Filename<br>Whole original file name including extension. i.e.: Smith_ED_Fig1.jpg | Figure/Table Legend<br>If you are citing a reference for the first time in these legends, please include all new references in the main text Methods References section, and carry on the numbering from the main References section of the paper. If your paper does not have a Methods section, include all new references at the end of the main Reference list. |
|---|---|---|---|
| Extended Data Fig. 1 | Analysis of auxin signalling and PIN polarity in lateral root columella cells | Roychoudhry_Supp Fig1.jpeg | (A) Ratio of nuclear R2DII signal across upper and lower epidermal cells in lateral roots at GSA (control) and reorientated upwards and downwards. Images were taken 90 mins post reorientation Bars represent standard error of mean nuclear fluorescence. n = 12-15 roots for each orientation from 3 biologically independent experiments. One way ANOVA revealed F stat (2) = 22.25654 with a p value = 0.001346. (B) Statistical analysis using pairwise two-tailed T tests revealed no significant difference in mean nuclear fluorescence of TIR1/AFB:Venus in atrichoblast cells on the upper and lower side of stage III lateral roots. n = 39-51 nuclei analysed for each transgenic line across 3 biologically independent experiments. (C) Outer membranes (white arrowheads) of upper and lower cells of the central columella used for quantification of PIN polarity in a single stack of a PIN3:GFP lateral root. Scale bar = 5 µm. (D) Quantification of PIN3/7::GFP fluorescence levels in plasma membranes of columella cells from stage III lateral and primary roots. n = 21-25 roots for each transgenic line quantified from 3 biologically independent experiments. Pairwise two tailed T-tests revealed no significant differences in membrane fluorescence levels. |

| | | | |
|---|---|---|---|
| Extended Data Fig. 2 | Quantification of the kinetics of gravitropic response in lateral roots of single and multiple *pin* mutants | Roychoudhry_Supp Fig2.jpeg | (A) Schematic representation of seedling reorientation for analysis of reorientation kinetics in WT and *pin* mutants. Plates were reoriented by 30$^{o}$ angles and tip angles of roots placed above and below their GSA (denoted in blue) were quantified at specified time intervals. (B) Reorientation kinetics of 12-day-old lateral roots in the *pin4pin7* double mutant. *pin4pin*7 lateral roots bend downwards rapidly, but show delayed upward bending presumably due to the loss of PIN7. (C,D) Reorientation kinetics of stage III lateral roots in the PIN3:GFP (C) and PIN7:GFP (D) transgenic lines. Lateral roots return to their original GSA in approximately 6 hours after reorientation in both directions. (B-D) n = 17-21 lateral roots at each time point from 3 biologically independent experiments (E,F) PIN polarity changes in 12-day old lateral roots reorientated in upward and downward directions. (E) PIN3:GFP and PIN7:GFP are predominantly dipolar (PIN3) and apolar (PIN7) in lateral roots at their GSA (right panels). In lateral roots reorientated below their GSA, both PIN3 and PIN7 polarise towards the upper side of columella cells (middle panels) whereas in roots displaced above their GSA, both PINs polarise towards the lower side of columella cells (left panels). White arrowheads indicate polar localisation of PIN:GFP signal. Scale bar = 5 µm. n = 12-15 roots at each reorientation from 3 biologically independent experiments. One way ANOVA revealed F stat (2) = 4.5096 with a p value = 0.0201 for PIN3:GFP and F stat (2) = 10.4650 with a p value = 0.0004 for PIN7:GFP. (G,H) Quantification of |

| | | | |
|---|---|---|---|
| | | | upper/ lower mean PIN3/7:GFP signal across external columella cell membranes in lateral roots at GSA and reorientated upwards and downwards at defined angles. Negative angles denote reorientation below GSA. Bars represent standard error of the means. (I) PIN2:GFP signal is not differentially expressed across upper and lower sides of lateral roots (right panel). Scale bar = 20 µm. (J) Quantification of PIN2:GFP upper/lower epidermal signal in trichoblasts across upper and lower epidermal cell files. Bars represent standard error of the means. |
| Extended Data Fig. 3 | Phosphorylation influences membrane retention kinetics and polarity of PIN proteins in lateral root columella cells | Roychoudhry_Supp Fig3.jpeg | A) Schematic representation of the 'flip' assay designed to study PIN membrane retention kinetics using vertical stage microscopy. (B, C) The PIP1;4:YFP (Wave11_Y) plasma membrane marker remains apolar in columella cells at their GSA (0 mins) or 30 mins after 'flipping'. Scale bar = 5 µm. (C) Ratio of PIP1;4:YFP plasma membrane polarity in lateral root columella cells at GSA and 30 mins post 'flipping'. n=12-15 roots for each time point from 3 biologically independent experiments. (D) Quantification of GSA phenotypes in lateral roots of 12-day-old PIN3:YFP S>A and S>D phosphovariant lines. (E) Quantification of lateral root GSA in the 12-day-old seedlings of PIN3:YFP D6PK phosphovariant line (PIN3:S45A:YFP). n = 15-21 roots for each genotype from 3 biologically independent experiments for (D) and (E). One way ANOVA with an F stat (2) = 7.7295 revealed a p value = 0.0026 for (D) while, a two tailed T-test revealed no significant differences were observed as compared to the PIN3:YFP control (E). (F) Expression of PP2AA/RCN1 |

| | | | |
|---|---|---|---|
| | | | phosphatase subunit and the PID/WAG kinase family in primary and lateral roots. *RCN1::RCN1:GFP* is expressed in both, the primary and lateral root columella cells (left upper and lower panels). In contrast *PID::PID:VENUS* and *WAG1::GUS* are not expressed in the primary or lateral root columella (Centre upper and lower panels). *WAG2::GUS* is absent from the primary root columella, but strongly expressed in the lateral root columella. Scale bar = 30 µm. The experiment was repeated independently three times with similar results. |
| Extended Data Fig. 4 | PIN3 dephosphorylation via RCN1 regulates lateral root GSA | Roychoudhry_Supp Fig4.jpeg | (A,B) Effect of 50 nM auxin treatment on *rcn1* (A) and *wag1wag2* (B) mutant lateral roots. *rcn1* lateral roots are unaffected by auxin treatment. *wag1wag2* lateral roots adopt a more vertical orientation upon auxin treatment. n = 12-15 roots per genotype per treatment for (A) and (B). One way ANOVA revealed an F stat (3) of 18.0109 and a p value = $5.09X10^{-6}$ for (A) and an F stat (3) = 10.1844 and a p value = 0.0002 for (B). (C,D) Upper/lower membrane ratios of PIN3:GFP in the columella cells of the *rcn1* and *pid*$^{+}$*wag1wag2* mutants. PIN3:GFP polarity is shifted to the upper columella membrane in the *rcn1* background but remains unaffected in the *pid*$^{+}$*wag1wag2* background. n = 24-27 roots for each genotype from 3 biologically independent experiments for (C) and (D). Data was statistically analysed using a two tailed T-test. (E) Expression of *ARL2::GFP* in lateral root columella cells. Scale bar = 50 µm. (F) Auxin treatment (50 nM IAA) shifts the lateral root GSA of *ARL2::RCN1 rcn* lateral roots to a significantly steeper orientation. n = 12-15 roots for each genotype |

| | | | |
|---|---|---|---|
| | | | per treatment from 3 biologically independent experiments. One way ANOVA revealed an F stat(3) value = 15.8911 with a p value = $3.67X10^{-7.}$ (G) Quantification of PIN3:GFP fluorescence in the columella cell plasma membranes in WT and mutant backgrounds. Fluorescence levels did not significantly differ between mutants and their WT controls. n = 22-30 per genotype from 3 biologically independent experiments. (H) Stage III lateral roots in the *rcn1* mutant background reorientate upwards to their original GSA in approximately 4 hours, while downward reorientation is delayed. (I) Stage III lateral roots of WT Ws plants reorientate both upwards and downwards in 6 hours. (J) In contrast, overexpression of *RCN1* in the columella in the WT Col-0 background leads to rapid downward reorientation of stage III lateral roots. (K) However, expression of *RCN1* in the *rcn1* mutant background restores reorientation kinetics of stage III lateral roots to a similar pattern as Ws. Data represent average values from 3 independent experiments. Bars represent standard errors of the means. with 6-8 roots reorienting in each direction per experiment per time point |
| Extended Data Fig. 5 | Effect of auxin treatment on *RCN1* expression and protein stability | Roychoudhry_Supp Fig5.jpeg | A,B) Effect of auxin treatment for 4 hours on *RCN1::RCN1:GFP* (*PP2AA::PP2AA:GFP* translational reporter line) primary root columella cells. Auxin treatment leads to a significant increase in RCN1:GFP signal levels. n = 15-21 roots from 3 biologically independent experiments. Statistical analysis was performed using a two tailed T-test. Scale bar = 20 µm. Red dashed lines represent area of columella signal |

| | | | |
|---|---|---|---|
| | | | quantification in (A). (C) Effect of 50 nM IAA on *RCN1* transcript levels in lateral root columella cells. No significant increase in *RCN1* levels occurred over an 8 hour time course. Data represent averages from 3 independent experiments with 7-8 root tips harvested for each time point per experiment. Bars represent standard error of the means. (D,E) Treatment with 50 nM IAA or 5F-IAA results in a shift in PIN3:GFP polarity towards the lower side of the columella cell, but has no effect on PIN7:GFP polarity. n = 12-15 roots per treatment from 3 biologically independent experiments. One way ANOVA revealed an F stat(5) value = 4.9116 with a p value = 0.0130. |
| Choose an item. | | | |
| Choose an item. | | | |
| Choose an item. | | | |
| Choose an item. | | | |
| Choose an item. | | | |

| Item | Present? | Filename<br>Whole original file name including extension. i.e.: Smith_SI.pdf. The extension must be .pdf | A brief, numerical description of file contents.<br>i.e.: *Supplementary Figures 1-4, Supplementary Discussion, and Supplementary Tables 1-4.* |
|---|---|---|---|
| Supplementary Information | No | | |
| Reporting Summary | Yes | Kepinski Flat RS.pdf | |
| Peer Review Information | No | *OFFICE USE ONLY* | |

| Type | Number<br>Each type of file (Table, Video, etc.) should be numbered from 1 onwards. Multiple files of the same type should be listed in sequence, i.e.: Supplementary Video 1, Supplementary Video 2, etc. | Filename<br>Whole original file name including extension. i.e.: *Smith_ Supplementary_Video_1.mov* | Legend or Descriptive Caption<br>Describe the contents of the file |
|---|---|---|---|
| Choose an item. | | | |
| Choose an item. | | | |
| Choose an item. | | | |
| Choose an item. | | | |
| Choose an item. | | | |
| Choose an item. | | | |

| Parent Figure or Table | Filename<br>Whole original file name including extension. i.e.: *Smith_SourceData_Fig1.xls,* or *Smith_ Unmodified_Gels_Fig1.pdf* | Data description<br>i.e.: Unprocessed western Blots and/or gels, Statistical Source Data, etc. |
|---|---|---|
| Source Data Fig. 1 | Source gel images for Fig 4G.pdf | Unprocessed gel shown in Fig 4G and Unprocessed loading control gel shown in Fig 4G |
| Source Data Fig. 2 | | |
| Source Data Fig. 3 | | |
| Source Data Fig. 4 | | |
| Source Data Fig. 5 | | |
| Source Data Fig. 6 | | |
| Source Data Fig. 7 | | |
| Source Data Fig. 8 | | |
| Source Data Extended Data Fig./Table 1 | | |

| | | |
|---|---|---|
| Source Data Extended Data Fig./Table 2 | | |
| Source Data Extended Data Fig./Table 3 | | |
| Source Data Extended Data Fig./Table 4 | | |
| Source Data Extended Data Fig./Table 5 | | |
| Source Data Extended Data Fig./Table 6 | | |
| Source Data Extended Data Fig./Table 7 | | |
| Source Data Extended Data Fig./Table 8 | | |
| Source Data Extended Data Fig./Table 9 | | |
| Source Data Extended Data Fig./Table 10 | | |

# Antigravitropic PIN polarization maintains non-vertical growth in lateral roots

Suruchi Roychoudhry[1], Katelyn Sageman-Furnas[1†], Chris Wolverton[2], Peter Grones[3§], Shutang Tan[3], Gergely Molnár[3α], Martina De Angelis[1], Heather L. Goodman[1‡], Nicola Capstaff[1#], James P.B. Lloyd[4], Jack Mullen[5], Roger Hangarter[6], Jiří Friml[3] & Stefan Kepinski[1*]

1. Centre for Plant Sciences, School of Biology, University of Leeds, UK
2. Ohio Wesleyan University, Ohio, USA
3. Institute of Science and Technology, Vienna, Austria
4. University of Western Australia, Australia
5. Department of Bioagricultural Sciences & Pest Management, Colorado State University, Fort Collins, Colorado, USA
6. Department of Biology, Indiana University, Bloomington, Indiana, USA

[§]Present address: Umeå Plant Science Centre, Umeå, Sweden

[†]Present address: Dept. of Biology, Duke University, North Carolina, USA

[‡]Present address: Tropic Biosciences Ltd, Norwich Research Park Innovation Centre, Norwich

[α]Present address: Department of Applied Genetics and Cell Biology, University of Natural Resources and Life Sciences (BOKU), Vienna, Austria

[#] Present address: Dept. of Science, Innovation and Technology, UK Government

*Correspondence: s.kepinski@leeds.ac.uk

**Abstract**

Lateral roots are typically maintained at non-vertical angles with respect to gravity. These gravitropic setpoint angles (GSAs) are intriguing because their maintenance requires that roots are able to effect growth response both with and against the gravity vector, a phenomenon previously attributed to gravitropism acting against an antigravitropic offset mechanism. Here, we show how the components mediating gravitropism in the vertical primary root—PINs and phosphatases acting upon them—are reconfigured in their regulation such that lateral root growth at a range of angles can be maintained. We show that the ability of Arabidopsis lateral roots to bend both downward and upward requires the generation of auxin asymmetries and is driven by angle-dependent variation in downward gravitropic auxin flux acting against angle-independent upward, antigravitropic flux. Further, we demonstrate a symmetry in auxin distribution in lateral roots at GSA that can be traced back to a net, balanced polarization of PIN3 and PIN7 auxin transporters in the columella. These auxin fluxes are shifted by altering PIN protein phosphoregulation in the columella, either by introducing PIN3 phosphovariant versions or via manipulation of levels of the phosphatase subunit PP2A/RCN1. Finally, we show that auxin, in addition to driving lateral root directional growth, acts within the lateral root columella to induce more vertical growth by increasing RCN1 levels, causing a downward shift in PIN3 localisation, thereby diminishing the magnitude of the upward, antigravitropic auxin flux.

## Introduction

Gravity is one of the most fundamental environmental signals controlling plant development and certainly the most constant. The capacity for gravity-directed growth, known as gravitropism, ensures that shoots typically grow upwards and roots grow downwards, allowing light interception and gas exchange above ground, and water and nutrient uptake below. These processes of resource capture are enhanced enormously by the production of

lateral root and shoot branches that grow out from the main root-shoot axis at non-vertical angles. Importantly, these branches are often maintained at specific angles with respect to gravity, independently of the main or parent axis from which they originate. These patterns of growth in primary and lateral organs are most easily understood in the context of the gravitropic setpoint angle (GSA) concept[1]. The GSA is the angle at which an organ is maintained with respect to gravity by the action of gravitropism. Vertically-growing organs have a GSA of 0º if they are growing towards the centre of the Earth and 180º if growing away, with non-vertical branches having GSAs between these two extremes.

To alter growth according to gravity, plant organs must have the capacity to perceive their orientation within the gravity field and to regulate elongation on their upper and lower sides differentially. These processes are well described by the starch-statolith model of graviperception and the Cholodny-Went model of tropic growth. In the first, the sedimentation of starch-rich amyloplasts within specialised statocyte cells provides information on the organ's angle with respect to gravity[2-4]. This information is translated into tropic growth through the asymmetric redistribution of the hormone auxin to the lower side of the organ[5-9] . Here, according to the Cholodny-Went model, auxin inhibits cell elongation in the root and promotes cell elongation in the shoot, driving downward and upward growth respectively[5,6].

The starch-statolith and Cholodny-Went models are linked by the action of the PIN family of auxin efflux carrier proteins and in particular, PIN3 and PIN7 (Friml *et al*., 2002; Kleine-Vehn *et al*., 2010; Rakusova *et al*., 2011). In Arabidopsis, both PIN3 and PIN7 are expressed in the columella statocyte cells where their subcellular distribution is dependent upon the orientation of the root tip. In a primary root growing vertically, PIN3 and PIN7 localization is essentially apolar but upon gravistimulation, both PIN3 and PIN7 can become rapidly relocalised to accumulate on the lateral, lower-most face of the columella cells, increasing the downward flux of auxin[7,10,11].From the root cap, auxin is transported shootward by PIN2

via the epidermis to the elongation zone (EZ) where cell expansion is regulated[12-14].Thus together, the starch-statolith and Cholodny-Went models, with the more recent addition of PIN-based auxin transport, are sufficient to account for the maintenance of the vertical growth typically observed in the primary root and shoot.

Non-vertical GSAs present an intriguing problem because in order to maintain a non-vertical growth angle, root and shoot branches must by definition have the capacity to reorient their growth both with and against gravity[15-17]. It has previously been shown that non-vertical GSAs are the result of an auxin-dependent antigravitropic offset (AGO or simply, offset) mechanism that counteracts the underlying gravitropic response in root and shoot branches such that stable, angled growth occurs when both growth components are balanced[16]. Using auxin treatment and mutants affected in either auxin homeostasis or response, it was also shown that auxin induced more vertical GSAs by diminishing the relative magnitude of the AGO[16].

The fact that AGO activity is auxin-dependent hints at a mechanism involving Cholodny-Went-type tropic response. Consistent with this idea, mutation of the columella-expressed auxin efflux carriers PIN3, PIN4, and PIN7 has been shown to affect lateral root GSA[18,19]. Further, these PIN proteins also show specific expression patterns throughout the development of the lateral root[18-20]. In Arabidopsis, lateral roots (LRs) emerge at a near horizontal orientation (stage I/type 1) and following the development of differentiated columella and a distinct elongation zone that marks the acquisition of gravicompetence, undergo a brief period of downward growth (stage II/type 2)[15,18,19,21]. From this point, lateral roots gain the capacity to stably maintain non-vertical GSAs and gradually transition through progressively more vertical GSA states (stage III-V/type 3-6). Stage III, sometimes referred to as the plateau phase, is particularly important in determining the extent of radial expansion of the root system[15,18]. PIN3:GFP expression in the columella is apparent from stage I onwards but begins to decline after stage III. In contrast, PIN4:GFP and PIN7:GFP

are undetectable in emerging lateral roots (stages I and II), with PIN7 expression in the columella becoming apparent in stage III and PIN4 detected in the columella from ~stage IV onwards[18,19,22]. Based on these distinctive expression patterns it was suggested that non-vertical GSAs might simply be the result of reduced gravitropic competence, arising from the fact that PIN protein expression levels in the columella of the lateral root are lower than those in the primary root[18,19]. While these spatiotemporal PIN expression patterns are likely to be highly relevant to lateral root GSA regulation, a model based solely on a lack of gravitropic competence is incompatible with the data supporting the GSA concept, most strikingly, the capacity of lateral roots to grow *upwards* to regain their GSA.

Here we have used molecular and genetic tools to reveal the mechanisms controlling GSA in the Arabidopsis lateral root. We show that GSA maintenance is underpinned by the control of both upward antigravitropic and downward gravitropic auxin fluxes in a manner consistent with the Cholodny-Went model. Specifically, we show that the ability of lateral roots to bend both downward and upward to maintain GSA is driven by cell elongation control on the lower side of the reorientating root. This organ-level behaviour is consistent with response to the observed angle-dependent variation in downward gravitropic auxin transport, where the magnitude of flux decreases closer to the vertical, acting against response to an upward, antigravitropic auxin flux that is more or less constant for a given GSA. These patterns of auxin distribution in the root tip are dependent on the subcellular localization of PIN3 and PIN7, which not only mediate gravitropic response, but also constitute the antigravitropic offset. In this context, growth at GSA is characterised by a net balanced capacity for upward and downward PIN-mediated auxin transport from the lateral root columella. Finally, we show that the protein phosphatase 2A subunit ROOTS CURL IN NPA1 (RCN1) acts upstream of PIN3 to promote an upper to lower side shift in the polarity of PIN3, but not PIN7, and further that auxin induces more vertical GSA in lateral roots by increasing RCN1 levels in the columella, thereby diminishing the magnitude of the upward, AGO auxin flux.

146

147 ## Results

148

149 **Gravitropic auxin transport in the Arabidopsis lateral root is offset by an antagonistic**
150 **auxin flux**

151 The control of auxin distribution across the root tip is central to gravitropism and the
152 maintenance of a typically vertical GSA in the primary root. To explore the role of auxin
153 transport in the maintenance of non-vertical GSAs, we tested the effect of the auxin
154 transport inhibitor NPA[23] on both upward and downward gravitropic growth in reorientated
155 lateral roots. In these experiments, lateral roots treated with either 0.2 μM or 0.4 μM NPA
156 failed to return to their original GSA after 24 hours following rotation by 30º either above or
157 below their GSA, albiet adopting a more vertical GSA. (Fig. 1A, B). At both concentrations,
158 the growth rates of lateral roots, although reduced, are not significantly different from the
159 wild type in our growth conditions (Fig. 1C) (Roychoudhry *et al*., 2013). These data therefore
160 indicate that auxin transport is necessary for both upward and downward gravity induced
161 growth curvatures.

162

163 To analyse auxin distribution and response in lateral roots growing at their GSA, and
164 following gravistimulation above and below their GSA, we used the reporters DII-Venus and
165 the ratiometric DII-Venus variant, R2D2[24,25]. In lateral roots growing at their GSA, these
166 reporters indicated no significant difference in auxin levels between the upper and lower
167 halves of lateral roots (Fig. 1D, E; Fig. S1A). The inference of auxin levels from DII-Venus
168 and R2D2 in this context is further supported by the lack of variation in TIR1/AFB auxin
169 receptor levels across the lateral root, quantified by TIR1:Venus, AFB1:Venus, AFB2:Venus
170 and AFB3:Venus translational reporter expression (Fig. S1B)[26]. In lateral roots reorientated
171 above their GSA (and bending downwards), quantification of DII-Venus (Fig. 1D, E) and
172 R2D2 (Fig. S1A) signals 90 mins post reorientation indicated higher levels of auxin

accumulation on the lower side of lateral roots (Fig. 1D, E; Fig. S1A). Conversely, in roots displaced below their GSA (and thus bending upwards), DII-Venus (Fig. 1 D, E) and R2D2 (Fig. S1A) signals indicated higher levels of auxin accumulation on the upper side of the lateral root, in the direction of tropic growth. Together, these data indicate that the maintenance of non-vertical GSAs is auxin transport-dependent and entirely compatible with the Cholodny-Went model of tropic growth.

To understand how these patterns of auxin distribution in reorientated lateral roots relate to the asymmetric cell elongation driving tropic curvature, we measured atrichoblast epidermal cell lengths across the upper and lower sides of stage III lateral roots both at GSA and following reorientation. In keeping with the lack of auxin asymmetry in lateral roots growing at GSA, we found that there were no significant differences in cell lengths between the upper and lower sides of the root (Fig. 1F, G). In downward bending lateral roots, epidermal cells on the lower side of the root were significantly shorter than those at the upper side, consistent with the asymmetric auxin accumulation in these cells and resulting auxin-mediated growth inhibition[27] in the lower half of the root (Fig. 1F, G). In upward bending roots, we observed that the cells on the lower side of the root were significantly longer than those on the upper side, and, interestingly, they were also longer than epidermal cells in roots growing at their GSA (Fig. 1F, G). Importantly, epidermal cells on the upper side of lateral roots undergoing either upward or downward tropic growth responses did not differ significantly in length. These data indicate that tropic growth in lateral roots is driven principally by control of cell elongation on the lower side of the root. This suggests a mechanism in which the maintenance of non-vertical GSAs depends upon stimulation angle-dependent variation in the gravitropic response on the lower side of the lateral root against a more constant and angle-independent antigravitropic component on the upper side.

To test if lateral root gravitropic responses are angle-dependent, we used a feedback-regulated system[28] to constrain stage III lateral roots at 30° and 45° below, and 30°, 45°,

60°, and 90° above their GSA. Constraint at 30° above or below GSA (mean GSA = 63°, SD = 7°) elicited almost identical rates of downward and upward bending respectively (Fig. 1H) Increasing the angle of reorientation to 45° above GSA led to a more than doubling of the rate of curvature (Fig. 1D), confirming that similar to primary roots[28],lateral roots are able to respond to gravity in an angle-dependent manner. Using the DII-Venus reporter, we found that these differences in angle-dependent reorientation kinetics were reflected in the magnitude of asymmetric auxin gradients across the upper and lower halves of lateral roots reoriented at different angles (Fig. 1I), providing a mechanistic explanation for the angle-dependent graviresponse.

**Non-vertical GSAs arise from a net symmetry in the polarity of PIN3 and PIN7 in the lateral root columella**

In Arabidopsis, lateral roots (LRs) emerge at a near horizontal orientation (stage I/type 1) and following the development of differentiated columella and a distinct elongation zone that marks the acquisition of gravicompetence, undergo a brief period of downward growth (stage II/type 2)[15,18,19,21] . From this point, lateral roots gain the capacity to stably maintain non-vertical GSAs and gradually transition through progressively more vertical GSA states (stage III-V/type 3-6). Of these phases of gravity-dependent growth, stage III, sometimes referred to as the plateau phase, is particularly important in determining the extent of radial expansion of the root system[15,18]. Both, PIN3 and PIN7 have been previously described to play a major role in translating information on the direction of gravity into asymmetric auxin fluxes by their gravity-induced polarization[7,10,11] and are expressed in stage III lateral roots, from which point GSAs are robustly maintained[18,20] . We therefore studied the localization and distribution of these PINs in Arabidopsis lateral roots growing at non-vertical GSAs using vertical-stage confocal microscopy[29]. In these experiments we measured the ratio of GFP signal in the plasma membranes on the upper and lower sides of outermost flanking cells (Fig. S1C). We found that PIN3, expressed mainly in the top two tiers of columella

229 cells, was targeted to both upper and lower plasma membranes, but was targeted to the
230 lower membrane in a slightly greater proportion of columella cells (Fig. 2A,C). PIN7 exhibited
231 a distinctly different pattern, being targeted to the upper plasma membrane in over 50% of
232 lateral roots analysed (Fig. 2B,C). In contrast with lateral roots at GSA, in primary roots
233 placed non-vertically (~45°), both PIN3 and PIN7 polarised predominantly towards the lower
234 side of the columella (Fig. 2A-C) 30 mins after reorientation, consistent with previous
235 studies[10]. We also quantified the mean plasma membrane fluorescence levels of PIN3:GFP
236 and PIN7:GFP in columella cells of stage III lateral and primary roots imaged under the
237 same settings. These experiments verified that there were no significant differences in PIN3
238 and PIN7 protein levels within lateral and primary columella cell membranes (Fig S1D, E).
239
240 Thus, PIN proteins in lateral roots have polarisation patterns that are distinct from those in
241 primary roots potentially providing an explanation for the symmetry in auxin distribution in
242 roots growing at their GSA.
243
244 To explore the significance of these cell biological observations, we examined the kinetics of
245 graviresponse in *pin3-3* and *pin7*-2 single and double mutants (Schematic of the
246 experimental setup is shown in figure S2A). Upon reorientation by 30° above and below
247 GSA, we found that lateral roots of the *pin3 pin7* double mutant were severely delayed in
248 returning toward their GSA compared to wild-type, although both upward and downward
249 tropic growth was still apparent (Fig. 2D,E). Because previous studies have shown that PIN4
250 expression domains expand into the columella in a compensatory manner in the *pin3* and
251 *pin7* mutant backgrounds[30], we also examined the graviresponse in the *pin3 pin4 pin7* triple
252 mutant and found the response to be virtually absent over a ten-hour timeframe (Fig. 2F).
253
254 The graviresponse kinetics of the *pin3* and *pin7* single mutants were particularly interesting.
255 We found that lateral roots of *pin3* seedlings reorientated upwards significantly faster than
256 downwards (Fig. 2H), while the reverse was true for lateral roots of *pin7* seedlings, albeit to

257 a lesser degree (Fig. 2I). In contrast, the graviresponse of *pin3* and *pin7* mutants
258 complemented with PIN3:GFP[31] and PIN7:GFP[32]was similar to WT Col-0 (Fig. S2C,D). We
259 also tested the response of the *pin3 pin4* double mutant which, similar to the *pin3* single
260 mutant, exhibited a much more rapid upward relative to downward tropic growth (Fig. 2G). In
261 contrast, the *pin4pin7* double mutant displayed rapid downward tropic growth, while upward
262 tropic growth was delayed, presumably due to the loss of PIN7 (Fig S2B). These data
263 indicate that the rapid upward bending associated with loss of PIN3 function requires PIN7
264 and are thus consistent with the observed subcellular polarity bias of PIN7 and to some
265 extent, PIN3.
266
267 To determine if the changes in auxin distribution observed in lateral roots under reorientation
268 (Fig. 1D, E, S1A) were reflected in shifts in PIN localization, we gravistimulated lateral roots
269 both above and below their GSA and examined PIN3:GFP and PIN7:GFP localization in the
270 columella by vertical-stage confocal microscopy. For lateral roots growing at their GSA, the
271 average upper/lower ratio for PIN3:GFP was approximately equal to one, whereas the ratio
272 was slightly higher (1.2) for PIN7:GFP (Fig. S2F, G) as described above (Fig. 2C).
273 Stimulation above GSA (downward bending) shifted the polarity of both PIN3 and PIN7 to a
274 predominantly basal localization, similar to that in primary roots (Fig. S2F, G). In contrast,
275 where lateral roots were reoriented below their GSA (upward bending), we observed an
276 increased signal at the upper plasma membrane relative to the lower side for both PIN3:GFP
277 and PIN7:GFP lateral roots (Fig. S2 F, G). Further, we observed that these shifts in PIN
278 polarity occurred in an angle-dependent manner, particularly in roots reoriented above their
279 GSA and bending downwards (Fig S2I,J). Thus, these changes in PIN3 and PIN7 polarity
280 are consistent with the observed R2D2 and DII-Venus data (Fig 1D, E, S1A) demonstrating
281 auxin redistribution during lateral root gravistimulation.
282
283 In addition to PIN3 and PIN7 activity in the columella, root graviresponse also requires the
284 action of PIN2 in the epidermis to drive the basipetal flow of auxin away from the root tip[33].

285 We therefore also studied PIN2:GFP expression in lateral roots growing at their GSA to
286 check for any differential expression of PIN2 that might contribute to the regulation of growth
287 angle. This analysis did not reveal differences in PIN2 expression between upper and lower
288 halves of lateral roots (Fig. S2K,L).
289
290 **PIN protein retention at the plasma membrane differs between upper and lower faces**
291 **of repolarising lateral root statocytes**
292
293 The subcellular distribution of PIN proteins is regulated via cycles of endocytosis and polar
294 or apolar redelivery to the plasma membrane[34]. In order to understand if there are
295 differences in PIN stabilisation within the upper and lower side membranes of lateral root
296 statocytes at GSA, we designed an assay to capture the dynamics of PIN protein
297 relocalisation during the gravity-induced repolarization of the cell. This involved 'flipping'
298 lateral roots growing at their GSA by 90° within their axis of growth, simply by moving from
299 vertical- to horizontal-stage confocal microscopic imaging and analysing, over time, the
300 faces of the statocyte that were previously 'up' and 'down' relative to gravity prior to the 'flip'
301 (Fig. S3A). For both PIN3:GFP and PIN7:GFP, the ratio of fluorescence signals at the faces
302 of the columella cells that were originally upper and lower with respect to gravity prior to the
303 experiment were recorded immediately after flipping and then at 30 minute intervals for 2
304 hours. Consistent with previous experiments (Fig. 2A-C), we found that immediately
305 following the flip, PIN3:GFP showed polarity distribution slightly towards the former lower
306 columella cell membrane, (Fig. 3A,B), while the opposite was evident for PIN7:GFP (Fig.
307 3C,D). Thirty minutes after 'flipping' we found that the majority of lateral roots now displayed
308 a significantly higher PIN3 and PIN7 signal at the former upper side of the cell (Fig. 3A-D).
309 This indicates that lower side PINs are endocytosed and polarised in the new direction of
310 gravity and statolith sedimentation at a faster rate as compared to upper side PINs.
311 Comparing the polarity distribution throughout the course of the experiments, we found that
312 for both PIN3 and PIN7, the proportion of lateral roots with upper polarity gradually

313 decreased, and the majority of lateral roots had acquired a symmetrical distribution across
314 both cell sides two hours after flipping (Fig. 3A-D). As a control, we performed the same
315 assay with another plasma membrane protein marker line, WAVE_11Y, consisting of the
316 plasma membrane protein PIP1;4 with a C-terminal YFP tag[35]. In lateral roots at their GSA,
317 there was no asymmetry in PIP1;4:YFP expression across the upper and lower membranes
318 of columella cells (Fig. S3B ,C). Additionally, 'flipping' did not lead to the generation of any
319 asymmetry of the YFP signal across the cell, suggesting that the ability to repolarize in the
320 direction of gravity is not a general property of plasma membrane proteins. Taken together,
321 these results indicate that there is differential stability or dynamics of PIN3 and PIN7 at the
322 upper versus lower plasma membranes of lateral root statocytes growing at GSA, with PIN3
323 and PIN7 being retained at the upper sides for longer.
324
325
326
327 **PIN phosphorylation affects PIN polarity and redistribution kinetics in lateral root**
328 **statocytes**
329 The phosphorylation of specific serine (S) residues in the cytoplasmic loops of PIN1 and
330 PIN2 proteins has been shown to induce localization to the shootward (upper) plasma
331 membrane in epidermal and vascular cells, while their dephosphorylation causes PINs to
332 localise to the rootward (lower) plasma membrane[33,36-38]. To explore whether
333 phosphorylation might play a role in the subcellular distribution of PINs within the lateral root
334 columella, we analysed lateral root GSA of plants expressing phosphovariant versions of
335 PIN3:YFP. In these lines, known PID/WAG- or D6PK-targeted serine residues were mutated
336 to either a nonphosphosphorytable (phosphodead) alanine (A)[39,40] or to the phosphomimic
337 amino acid aspartic acid (D) (Grones *et al.*, 2018). Previous studies have shown that
338 phosphorylation at the specific residues of S316, S317 and S321 for PID/WAG and S215
339 and S283 (annotated as S4 and S5) for D6PKs can affect the gravity-induced repolarization
340 of PIN3 in the root and hypocotyl respectively[39,40]. We found that lines in which the S316,

341 S317 and S321 PID/WAG sites of PIN3:YFP were mutated to alanine (PIN3S>A:YFP) had
342 more vertical lateral root GSAs, while the mutation of those same residues to aspartic acid
343 (PIN3S>D:YFP) induced lateral roots to grow at a more horizontal GSA than control
344 PIN3:YFP plants (Fig. S3D). In contrast, the mutation of D6PK phosphosites to alanine
345 (PIN3:S45A:YFP) had no effect on lateral root GSA (Fig. S3E).
346
347 To investigate the GSA phenotypes of these PIN3 phosphovariant lines we imaged lateral
348 roots growing at GSA and observed that, compared to native PIN3:YFP, the distribution of
349 PIN3S>D:YFP was shifted significantly towards the upper membrane of lateral root
350 columella cells, while that of PIN3S>A:YFP was shifted slightly, but not significantly towards
351 the lower membrane (Fig. 3E,F). We also performed flip assays using the PIN3:YFP
352 phosphovariant derivatives, which showed that the characteristic persistence of a stronger
353 PIN3 signal of the former upper side of lateral root statocyte at 30 minutes post-flip was lost
354 in the PIN3S>A:YFP line but retained in PIN3S>D:YFP (Fig. 3G,H)
355
356 The absence of a GSA phenotype in the D6PK phosphovariant line prompted us to focus on
357 the role of the PID/WAG kinases and PP2AA/RCN1 phosphatases in the regulation of PIN-
358 mediated transport from lateral root statocytes. Analysis of transcriptional and translational
359 marker lines showed that while PID and WAG1 were below the level of detection in primary
360 and lateral root columella cells, a third member of this family, WAG2 is expressed solely in
361 the lateral root columella (Fig. S3F). RCN1 is expressed in both primary and lateral root
362 columella cells (Fig. S3F). Interestingly, loss of RCN1 function in the *rcn1* mutant causes
363 lateral roots to grow with a significantly less vertical GSA (Fig. 3I), while the double loss-of-
364 function mutant *wag1 wag2* induces a more vertical lateral root GSA (Fig. 3J). These data
365 are therefore compatible with the PIN phosphovariant data and the idea that RCN1-
366 mediated phosphatase activity facilitates the ‘downward’ fluxes of auxin from lateral root
367 statocytes, and that kinases such as WAG2, and possibly others that target the PIN3
368 cytoplasmic loop, facilitate an opposite, ‘upward’ auxin flux.

369

370 **Auxin regulates lateral root GSA through a PIN3-specific phosphorylation module**

371 It has previously been shown that auxin treatment is able to shift lateral root GSA towards a
372 more vertical orientation[16,18,26]. We therefore hypothesised that auxin might affect lateral root
373 GSA by affecting PIN polarity, for example, by increasing the pool of dephosphorylated PINs
374 within the lateral root columella. This increase could be achieved either through an auxin-
375 mediated up-regulation of RCN1 expression or activity and/or down-regulation of the
376 opposing kinase expression or activity. To explore this possibility, we tested the effect of
377 auxin treatment on lateral root GSA in *rcn1* and *wag1 wag2*. *rcn1* lateral roots failed to
378 respond to auxin treatment (Fig. S4A), while the lateral roots of *wag1 wag2* double mutants
379 shifted to a more vertical GSA orientation, similar to wild-type (Fig. S4B), indicating that
380 auxin might control lateral root GSA through an RCN1-dependent pathway. We also
381 observed that PIN3:GFP polarity was shifted towards the upper plasma membrane in the
382 columella cells of the *rcn1* mutant, but remained unchanged from that of WT in the
383 *pid*$^{+}$*wag1wag2* mutant background (Fig S4C, D). Consistent with this idea, the
384 overexpression of *RCN1* driven specifically in the columella by the promoter of *ARL2*, a
385 columella-specific gene[41]. (Fig. S4E), in the Col-0 background led to a significantly more
386 vertical lateral root GSA phenotype (Fig. 4A). Indeed, this same *ARL2::RCN1* transgene was
387 able to rescue the horizontal GSA phenotype of *rcn1* lateral roots (Fig. 4B) and restore the
388 GSA shift response to auxin treatment in *rcn1* (Fig. S4F). Also*, rcn1* stage III lateral roots
389 reoriented upwards towards their GSA more rapidly (Fig. S4I, J), while those of *ARL2:RCN1*
390 reoriented downwards more quickly (Fig. S4I,K). Importantly, the protein levels of PIN3:GFP
391 did not change significantly from the WT control, in any of these mutant backgrounds (S4G).

392

393 To understand if auxin regulates lateral root GSA directly via RCN1 levels, we analysed the
394 effect of auxin on the abundance of an RCN1::RCN1:GFP translational reporter by confocal
395 microscopy. We found that treatment with 50 nM IAA for 4 hours significantly increased GFP
396 signal in both lateral and primary root columella cells (Fig. 4C,D; S5A, B). Analysis of *RCN1*

397 transcript levels in lateral root tips treated with 50 nM of IAA over a time course between 2
398 and 8 hours showed that auxin had no significant effect on *RCN1* expression compared to
399 mock-treated lateral roots (Fig. S5C), indicating that the effect of auxin on RCN1 protein
400 levels is post-transcriptional in nature. These data suggest that auxin is able to regulate
401 lateral root GSA through a signalling pathway that is dependent on RCN1 stabilisation or
402 enhanced translation.
403
404 Because the expression of RCN1 solely in the columella had the same effect as exogenous
405 auxin treatment on lateral root GSA, we decided to examine the polarity of PIN3:GFP and
406 PIN7:GFP within the columella cells of lateral roots either in the *ARL2::RCN1* background, or
407 treated with 50 nM of IAA or 5F-IAA for 24 hours, an auxin analogue acting specifically
408 through the TIR1 signalling pathway[42]. Under all of these conditions, we found that the
409 polarity of PIN3:GFP was significantly shifted towards the lower side of lateral root columella
410 cells relative to WT or mock controls (Fig. 4. E,F; Fig. S5D, E). In contrast, the overall
411 polarity of PIN7:GFP was unaffected both in the *ARL2::RCN1* background and by auxin
412 treatment (Fig. 4. E, F; Fig. 5D, E). These data underline the differences in the subcellular
413 targeting of PIN3 and PIN7 in the gravity-sensing cells. They also indicate that auxin can act
414 to induce more vertical lateral root GSAs by stabilising RCN1 in the columella, thereby
415 reducing the pool of phosphorylated PIN3 and hence the capacity for upward, antigravitropic
416 auxin flux from the lateral root tip. Consistent with these data, we found that RCN1/PP2A
417 could dephosphorylate the hydrophilic loop of PIN3 *in vitro* (Fig. 4G). The subsequent
418 reduction in upward auxin flux and the angle-dependence of graviresponse in the lateral root
419 means that the equilibrium between gravitropic and antigravitropic auxin fluxes occurs at a
420 smaller angle of displacement from the vertical, producing a steeper GSA.
421
422 **Discussion**
423 The ability of plants to maintain their lateral organs at specific GSAs appears to be a
424 complex problem requiring both the monitoring of multiple growth angles and the capacity to

425 reversibly control gravitropic responses both with and against the gravity vector[1,15]. Here we
426 have shown that non-vertical GSAs in lateral roots arise from the interaction of just two
427 phenomena—angle-dependent gravitropic response and an angle-independent
428 antigravitropic offset—mediated at the level of PIN phosphorylation via RCN1, in the gravity-
429 sensing columella cells (Fig. 5A,B).
430
431 The demonstration of quantitative, angle-dependent variation in lateral root gravitropic
432 response is significant because while the angle of growth is set by the magnitude of the
433 AGO, it is the capacity of gravitropic response to increase with displacement from the
434 vertical that provides a means to maintain that angle of growth. The central importance of
435 angle-dependence in the maintenance of non-vertical GSAs contrasts with its apparent
436 dispensability for achieving vertical growth in primary organs. Although angle-dependence
437 contributes to limiting overshooting in primary roots returning to the vertical following
438 displacement[28], it is perhaps more likely that the major adaptive significance of angle-
439 dependence as a phenomenon lies in its capacity to sustain gravity-dependent non-vertical
440 growth.
441
442 Our data have demonstrated that the maintenance of non-vertical GSAs in lateral roots,
443 including both upward and downward growth, is based entirely within a framework of PIN-
444 mediated auxin transport in the lateral root tip (Fig. 1C-F; Fig. S1F). Furthermore, because
445 the control of downward gravitropic and upward antigravitropic auxin fluxes from the
446 columella are dependent on the same molecular components, it is the relative magnitude of
447 each that determines angle of growth, independent of the overall levels of auxin and PIN
448 proteins at a given stage of lateral root development.
449
450 The concept of gravitropic and antigravitropic activities acting in tension to generate gravity-
451 dependent non-vertical growth becomes less abstract when thought of in the mechanistic
452 terms of the PIN proteins that mediate auxin efflux from the gravity-sensing columella cells.

453 PIN3 and PIN7 in the columella of stage III lateral roots growing at GSA have distinct polarity
454 patterns with PIN3:GFP polarising slightly to the lower columella cell membrane and
455 PIN7:GFP doing the opposite (Fig. 2A-C). This shifted polarity pattern for PIN7 is reflected
456 in the reorientation kinetics of single and double columella PIN mutants. Lateral roots of *pin3*
457 and *pin3 pin4* mutants display rapid upward-bending relative to downward bending, a
458 phenomenon that is lost in the absence of PIN7 (Fig. 2D, F; Fig. S2B). While these data
459 indicate that PIN3 and PIN7 make distinct contributions in mediating gravitropic and
460 antigravitropic auxin flux from the columella, they are not exclusive for one or the other. For
461 both PIN3:GFP and PIN7:GFP, reorientation either above and below GSA causes shifts in
462 polarity in lateral root gravity-sensing cells that are consistent with the observed changes in
463 auxin distribution in both downward and upward-bending roots (Fig. S2E,F).
464
465 During 'flip assays' in repolarising columella cells, both PIN3:GFP and PIN7:GFP were found
466 to persist longer on the former upper side of the statocyte relative to the lower side (Fig. 3A-
467 D). The rapid reduction in PIN3 and PIN7 from the former lower membrane of statocytes in
468 these assays (Fig. 3A-D) demonstrates that the loss of statolith-mediated gravitropic
469 stimulation is associated with a rapid reduction in auxin transport capacity relative to the
470 former upper side of the cell. This is an important finding because it is this response at the
471 cellular level that gives rise to the organ-level response of upward bending where a lateral
472 root is moved back towards the vertical, below its GSA.
473
474 In addition to accounting for differences in the kinetics of change in gravitropic and
475 antigravitropic activities, the disparity in PIN protein dynamics on the upper and lower sides
476 of columella cells also suggest a parsimonious model of cellular polarity that avoids the
477 requirement to specify 'up' and 'down' domains within the cell separately. If statolith
478 sedimentation simply defines a 'down' domain in each cell[43,44] , the remainder of the cell can
479 be said to be in a 'not-down' state. However, since auxin transport from the lateral plasma
480 membranes of the statocyte are perpendicular to the gravity vector, it is only the relative

481 magnitude of auxin transport from the down and the opposing not-down/up faces of the cells
482 that determine growth trajectory in the vertical plane.
483
484 Several molecular and genetic data indicate that the subcellular partitioning of PIN3 to down
485 and not-down regions of columella cells is regulated by the phosphorylation of sites within its
486 cytoplasmic loop, including those targeted by the PID/WAG class of AGC kinases[45]. At this
487 point we cannot distinguish between the effect of the serine to alanine mutations at residues
488 316, 317 and 321 of PIN3 as being to promote targeting to 'down' domains of the cell or to
489 inhibit their phosphorylation-dependent targeting to not-down domains. The same applies in
490 the case of the mutation of these residues to aspartic acid, in that the effect could be either
491 or both, the active targeting of phosphovariant PIN3:GFP to not-down domains or the
492 inhibition of its recruitment to down domains. Whatever the case, these data point to
493 regulatory events involving these phosphosites as being important for PIN protein targeting
494 in the gravity-sensing cells of the root and hence regulation of GSA[39,46] . This conclusion is
495 supported by the finding that the expression of the PIN phosphatase subunit RCN1 in the
496 lateral root columella sufficient to regulate GSA (Fig. 4A,B). In addition to inducing a
497 downward shift in GSA, the overexpression of *RCN1* in the columella also causes a
498 concomitant downward shift in PIN3:GFP but strikingly, not in PIN7:GFP, again highlighting
499 the differences in the subcellular targeting of these proteins (Fig. 4E,F). At this point the
500 molecular basis of the cell biological differences between PIN3 and PIN7 in lateral root
501 statocytes is not clear. The fact that the subcellular distribution of PIN7 in the columella is
502 unaffected by RCN1 activity suggests that the reason for the distinct upper side polarisation
503 of PIN7 is either not related to phosphorylation or at the very least, involves phosphorylation
504 of sites that are not subject to regulation by RCN1. For PIN3, although phosphorylation of
505 serines 316, 317 and 321 is functionally relevant to the control of its polarity in the columella,
506 we do not know if other phosphosites in its cytoplasmic loop, which are targeted by RCN1,
507 contribute to GSA control.
508

509 Previous work has shown that auxin treatment induces steeper GSAs in lateral roots[16,18].
510 Further, auxin levels in the lateral root tip increase as the lateral root grows out form the
511 main axis, providing an explanation for the increasingly vertical growth of older lateral and a
512 means for the integration of environmental signals controlling root growth angle[26]. Our data
513 show that RCN1 activity in the columella is part of the mechanism underlying this response
514 to auxin. *rcn1* lateral roots are almost entirely resistant to the effect of auxin on GSA (Fig.
515 S4A) and auxin treatment increases RCN1 protein levels in the columella (Fig. 4C,D;
516 S5A,B), inducing a downward shift in PIN3:GFP, but not PIN7:GFP (Fig. 4E,F), consistent
517 with the effects of *RCN1* overexpression. Together, these data provide compelling support
518 for the idea that control of RCN1 levels and hence PIN3 polarity in the columella is central to
519 auxin's ability to regulate lateral root GSA.
520
521 **Conclusion**
522 Our work has shown how the patterns of growth angle control observed in lateral roots arise
523 from the interaction of angle-dependent gravitropic response and angle-independent, auxin-
524 repressible antigravitropic offset, both mediated at the level of lateral root columella PIN
525 proteins. This represents a leap in our understanding of the mechanisms governing AGO
526 and of how non-vertical growth can be maintained in plant lateral organs.
527
528 Previously, other mechanisms contributing to growth angle control in the young lateral root
529 have been proposed[47]. Here, an asymmetry in cytokinin distribution towards the upper side
530 of stage II lateral roots reflecting the lower-side asymmetry in auxin distribution observed
531 during this early, post-emergence phase of growth (Waidman *et al*., 2019). In this model,
532 cytokinin inhibits the ability of young lateral roots to respond to gravity, thereby limiting
533 downward growth. This cytokinin-based mechanism pertains to the phase of growth that
534 precedes the capacity of roots to maintain GSAs[15,47] . and so would be expected to influence
535 the growth angle of the lateral root during the first ~0.2-0.5 mm of its growth[15,16,18,47].
536

537 Recent work has also emphasised that other signalling systems are very relevant to the
538 regulation of growth angle. Ogura *et al*. (2019)[22] used GWAS to identify a role for the
539 EXO70A3 complex in regulating root angle and root system depth through dynamic
540 modulation of the PIN4 auxin efflux transporter. This study is of particular interest because
541 PIN4 expression across accessions is correlated with rainfall patterns and drought
542 resistance, providing an evolutionary and adaptive link between root architecture control and
543 the environmental conditions. Other interesting studies have further elucidated the role of the
544 LAZY protein family in primary and lateral root gravitropism and growth angle regulation[48-52] .
545 For example, using molecular genetics and structural biology, Furutani *et al.* have
546 convincingly demonstrated that LAZY proteins interact with RLD proteins, a novel family of
547 regulators of PIN polarity, which in turn leads to the accumulation of PIN3 in lateral root
548 columella cells[52]. These new studies are important and have clearly identified new players in
549 the regulation of lateral root growth angle. The work presented here complements these
550 studies by providing an explanation for the defining property of GSA control, i.e. the capacity
551 to *maintain* an angle relative to gravity by means of both upward and downward tropic
552 response. In this respect, it will be interesting to understand how, for example, LAZY and
553 RLD protein activity integrates with the columella PIN-specific phosphoregulation
554 mechanism identified here. The partial preference for PIN3 to localise to the lower face of
555 columella cells (Fig. 2E) would be consistent with the fact that *lazy* and *rld* mutant lateral
556 roots display more horizontal GSA phenotypes but there is significant scope for deeper
557 mechanistic links to be uncovered.
558
559 Perhaps the most conspicuous open question at hand is a very old one, that of how statolith
560 sedimentation is turned into asymmetry in PIN localization and activity within statocytes. In
561 the context of GSA control, the question relates to understanding the basis of angle-
562 dependent graviresponse, which is so crucial to the maintenance of non-vertical GSAs. By
563 highlighting the evolutionary and adaptive significance of such phenomena, the model of

564 GSA control proposed here provides not only practical tools but also fresh approaches to
565 tackling these fascinating and important questions in plant biology.
566
567
568 **Materials and methods**
569 *Plant materials*
570 All Arabidopsis seed stocks are in the Col-0 background unless otherwise stated. R2D2[25]
571 is in the Utrecht background. The *pin3-3, pin7-2, pin3-5 pin7-1 [pin3 pin7], pin3-5 pin4-3*
572 *[pin3 pin4], pin3-5 pin4-3 pin7-1 [pin3 pin4 pin7], pin4-3 pin7-1 [pin4 pin7]* [7,32], PIN3:GFP,
573 PIN7:GFP[10]*, rcn1*[53], *wag1 wag2*[54], PIN3:YFP, PIN3S>A:YFP and PIN3S>D:YFP[39],
574 *RCN1::RCN1:GFP [PP2AA::PP2AA:GFP]*, *PID::PID:Venus*, *WAG1::GUS*, *WAG2::GUS*[36],
575 PIN3:S4S5A:YFP [and PIN3:YFP control][40], DII-Venu[24], *TIR1::TIR1:Venus,*
576 *AFB2::AFB2:Venus,* and *AFB3::AFB3:Venus*[26] lines have been described previously. Ws-
577 0 seeds were obtained from the Nottingham Arabidopsis Stock Centre. The *ARL2:RCN1*
578 construct was generated by cloning 2.5 kb of the *ARL2* promoter upstream of the *RCN1*
579 coding sequence using a multiplex gateway cloning strategy (Invitrogen) into a
580 pALLIGATOR V destination vector. The *ARL2::GFP* construct was generated by cloning
581 2.5 kB of the *ARL2* promoter sequence into a modified pGreen 0229 vector containing
582 GFP cloned upstream of a NOS terminator. Transformation of these constructs to
583 Arabidopsis was accomplished via *Agrobacterium tumefaciens* (strain GV3101)-mediated
584 infiltration by floral dip. The *pid*$^{+}$ *wag1 wag2* PIN3:GFP line has previously been
585 described[11]. PIN3:GFP in the *rcn1* and Ws backgrounds and *ARL2::RCN1* PIN3:GFP and
586 *ARL2:RCN1* PIN7:GFP lines were generated by crossing.
587
588 *Reorientation experiments*
589 12-day-old seedlings grown vertically on 120 mm square ATS media plates under light
590 and temperature regimes described above were reorientated by appropriate angles in

591 darkness. Images were captured automatically at described intervals using a Canon
592 700D digital camera and infra-red illumination using the 'Image Capture' software in OS
593 El Capitan on a 2013 MacBook Pro in order to nullify any phototropic effects. The angles
594 of stage III lateral root tips were measured using ImageJ (https://imagej.nih.gov) before
595 reorientation and subsequently at defined time intervals. The average GSAs of reoriented
596 root tips was plotted to generate the reorientation plots. 10-12 roots were used to quantify
597 average GSA at each time point for both upward and downward reorientations in each
598 experiment, and each experiment was repeated three times.
599
600 *Maintenance of constant gravistimulation and measurement of root orientation.*
601 Roots were illuminated with an infrared light-emitting diode (Radio Shack, Fort Worth, TX)
602 and imaged with a CCD camera interfaced to a computer via a frame grabber card
603 (Imagenation Corp., Beaverton, OR). A computer feedback system connected to a rotary
604 stage[28] was used to measure the orientation of the root apex and constrain it to that initial
605 orientation prior to gravistimulation by making corrections every 45 s. Following
606 reorientation, the root tip was constrained at the new orientation to maintain a constant
607 gravistimulus throughout the experiment. Gravitropic curvature was measured as the
608 rotation of the stage necessary to maintain the root tip at a constant orientation.
609
610 *qRT-PCR for RCN1 expression*
611 RNA was extracted from the lateral and primary root tips of 12 day-old wild-type Col-0
612 plants grown on ATS media overlaid with Sefar Nitex mesh using the Qiagen RNAeasy kit
613 according to the manufacturer's instructions. cDNA was synthesized from the isolated
614 RNA using oligo dT primers and Superscript II reverse transcriptase (Invitrogen). qPCR
615 was performed using the Bio-Rad CFX Connect Real-Time System (Bio-Rad). GAPDH
616 was used as an internal control.
617
618

619 *Analysis of lateral root GSA*

620 In our experimental conditions, stage III lateral roots are 0.5 - 3 mm in length and remain
621 at this stage for approximately 24 hours. Briefly, the angle that a 1 mm segment of a
622 stage III lateral root made with the vertical was quantified . GSA was plotted as the angle
623 of this segment. At least 6 roots were quantified for each experiment. Each experiment
624 was repeated three times.

625

626 *Confocal microscopy*

627 10-12 day old marker seedlings grown on ATS or half MS media in standard tissue
628 culture conditions (20-22 $^{o}$C 16h day, 8h dark) were imaged at 20X resolution with the
629 480 nm and 540 nm lasers using a Zeiss LSM 710 inverted confocal microscope. For
630 vertical stage confocal microscopy and gravistimulation, the imaging setup described in
631 Von Wangenheim *et al.*, (2017)[29] was used. All laser power and gain settings were
632 consistent across images. Briefly, PIN:GFP markers were imaged using a series of Z
633 stacks and fluorescence intensity across external membranes was quantified using
634 ImageJ as described in Grones *et al.*, 2018[39]. For flip assays, root tips were
635 counterstained with PI prior to imaging. A series of stacks across the central columella
636 was captured for both, the GFP and PI channels. Using the 'Plot profile' function in
637 ImageJ, the X axis point of maximal intensity in the PI channel was identified as the cell
638 wall. The GFP fluorescence was measured and calculated across each cell membrane on
639 either side of the cell wall. Each experiment was performed three times with at least 6
640 roots for each experiment. Representative images were also taken for individual cells
641 across the series of time points. The images shown are generated using the 'Sum of
642 stacks' function with the '16 colours' LUT. For cell length quantification, wild-type Col-0
643 plants on ATS grown on ATS media were reorientated for a period of 6 hours. The entire
644 root system was mounted on a glass slide and counter stained with propidium iodide prior
645 to imaging the elongation zone of stage III lateral roots. The length of 3-4 fully elongated
646 cells epidermal atrichoblast cells on either flank of the root was quantified using ImageJ.

647 The experiment was performed three times with at least 6 roots at each orientation per
648 experiment. For DII-Venus and R2D2, excluding the lateral root cap, nuclear fluorescence
649 was measured in ten consecutive epidermal cells within the two outermost flanking cell
650 files, beginning from the root tip for each root. Experiments were performed three times
651 with at least ten root tips for each orientation per experiment. For R2D2, nuclear
652 fluorescence intensity was measured across both GFP and mTOMATO channels. For
653 each nucleus, the ratio of GFP/mTOMATO signal was determined. Geometric means and
654 standard errors of the ratios were calculated for both young, and older lateral roots.
655 Student's T-test was performed to evaluate statistical differences between the geometric
656 means of the data obtained.
657
658 *Recombinant protein expression and purification from Escherichia.coli*
659 Coding sequences of RCN1, PID, and PIN3HL were cloned into the pET28a vector
660 (Novagen) by the restriction enzyme digestion method. Recombinant His-tagged proteins,
661 including His-RCN1, His-PID and His-PIN3HL, were expressed in a BL21 (DE3) strain
662 with induction by 0.5 mM IPTG (isopropyl β-D-1-thiogalactopyranoside) for 16h at 12°C.
663 500 mL of *E. coli* culture was harvested by centrifuge, resuspended in 35 mL 1 × TBS (50
664 mM Tris-Cl, 150 mM NaCl; pH 7.6) buffer, and was then subjected to sonication. Proteins
665 were then purified using Ni-NTA His binding resin (Thermo Scientific) following the
666 manufacturer's instruction. Eventually, the resultant protein samples were checked by
667 SDS-PAGE (sodium dodecyl sulfate-polyacrylamide gel electrophoresis) and visualized
668 by Coomassie brilliant blue (CBB) staining.
669
670 *Isolation of the PP2A/RCN1 complex from plant extracts*
671 35 mL lysate of His-RCN1 from 500 mL of *E. coli* culture was incubated with 1.5 mL Ni-
672 NTA His binding resin (Thermo Scientific) for 30 min, and the supernatant was discarded.
673 At the same time, 3 g Col-0 seedlings were homogenized into plant extraction buffer (20
674 mM Tris-HCl, pH 7.5, 150 mM NaCl, 0.5% Tween-20, 1 mM EDTA, 1 mM DTT)

675 containing a protease inhibitor cocktail (cOmplete, Roche) and a protein phosphatase
676 inhibitor tablet (PhosSTOP, Roche). The protein-bound resin was then incubated with
677 protein extracts for 2h at 4°C. Afterwards, the column was washed twice with 10 mL wash
678 buffer (1× TBS+20 imidazole), and then eluted with 1 mL elution buffer (1× TBS+250
679 imidazole) by three times. Protein samples were checked by SDS-PAGE and visualized
680 by CBB staining.
681
682 *In vitro* (de)phosphorylation assay with γ-[$^{32}$P]-ATP
683 *In vitro* (de)phosphorylation assays with γ-[$^{32}$P]-ATP were performed as previously
684 described with some modifications. Recombinant His-PID (1 μL), His-PIN3HL(10 μL) with
685 different concentrations of PP2A were incubated in the reaction buffer [50 mM Tris-HCl
686 pH 7.5, 10 mM $MgCl_2$, 1 mM ATP (adenosine 5'-triphosphate), and 1 mM DTT] at the
687 presence of 5 μCi [γ-$^{32}$P]-ATP (NEG502A001MC, Perkin-Elmer) at 25°C for 90 min.
688 Afterwards, reactions were stopped by adding the SDS loading dye. The resultant
689 samples were subjected to SDS-PAGE. Gels were developed with a phosphor-plate
690 overnight and the signal was eventually imaged with a Fujifilm FLA 3000 plus DAGE
691 system.
692
693 *Statistics and reproducibility*
694 All experiments were repeated independently three times. All statistical data were tested
695 for normality using Kolmogorov-Smirnoff's test and analysed using either a pairwise two
696 tailed T-test or one way ANOVA followed by Tukey's HSD posthoc tests. Obtained p
697 values are presented in each figure, and values for 'F' along with degrees of freedom,
698 and p values from ANOVA tests are described in the appropriate figure legends. Data are
699 presented as individual data points using 'R'.
700
701 **Data availability**

Figures 1-4 in the main manuscript have associated raw data in the form of multiple images used for analysis and generation of graphs. There is no restriction on data availability. All data generated in this study are included within the main text and supplementary information. All experimental materials generated in this work are available from the corresponding author upon request. Open access datasets are available at 10.5281/zenodo.8019901.[55]

**Acknowledgments**

We thank Dolf Weijers, Claus Schwechheimer, and Remko Offringa for generous sharing of published and unpublished materials and Patrick Masson for advice on the use of the *ARL2* promoter. We are grateful to Marta Del Bianco and Ottoline Leyser for critical reading of the manuscript. This work was supported by the BBSRC (grants BB/N010124/1 and BB/R000859/1 to SK), the Gatsby Charitable Foundation and the Leverhulme Trust.

**Author contributions**

S.R performed the majority of experiments and analysed the data except: K.S-F generated and analysed the R2D2 data and constructed the *ARL2:GFP* transgenic line. M.D.A generated the PIN3:GFP lines in the *rcn1* and Ws backgrounds. H.L.G and N.C analysed GSA phenotypes of the *wag1 wag2* mutants. P.G and J.F generated the PIN3:YFP phosphovariant lines. S.T and G.M performed the *in vitro* phosphorylation assays. J.P.B.L assisted with data analysis and generation of graphical data. C.W, J.M and R.H generated the lateral root angle-dependence data. J.F provided critical experimental suggestions and feedback on the draft manuscript. S.R. and S.K wrote the manuscript. All authors commented on and approved the manuscript.

**Competing interests**

The authors have no competing interests to declare.

| Name | Purpose | Sequence (5' to 3') |
|---|---|---|
| B5r *RCN1* | *RCN1* entry clone generation | GGG GAC AAC TTT GTA TAC AAA AGT TGT AAT GGC TAT GGT AGA TGA ACC G |
| *RCN1* B2 | *RCN1* entry clone generation | GGG GAC CAC TTT GTA CAA GAA AGC TGG GTT TCA GGA TTG TGC TGC TGT GG |
| B5r *WAG2* | *WAG2* entry clone generation | GGG GAC AAC TTT GTA TAC AAA AGT TGT AAT GGA ACA AGA AGA TTT CTA TTT CCC TGA C |
| *WAG2* B2 | *WAG2* entry clone generation | GGG GAC CAC TTT GTA CAA GAA AGC TGG GTT TTA AAC GCG TTT GCG ACT CGC |
| B1 *ARL2* | *ARL2* entry clone generation | GGG GAC AAG TTT GTA CAA AAA AGC AGG CTT TTT AAA CTG ATT ACA AAA ATC TTA TAT AC |
| *ARL2* B5 | *ARL2* entry clone generation | GGG GAC AAC TTT TGT ATA CAA AGT TGT TGT TCA ATA ACA GGT TTT TGT TTC CCA GTT TG |
| qRCN1 Fwd | *RCN1* qPCR Fwd primer | AGT GTT TGG TGG ACC TGA GC |
| qRCN1 Rev | *RCN1* qPCR Rev primer | GAT TGT GCT GCT GTG GAA CC |

730 Table 1: List of primer sequences used in this study.

731

732 **Figure legends**

733 **Figure 1. Lateral root graviresponse is angle-dependent and driven by auxin**

734 **transport-dependent auxin asymmetry** (A,B) Mean GSA of mock and NPA treated

735 stage III lateral roots growing at GSA and 24 hrs after reorientation by 30°. Treatment

736 with 0.2 μM and 0.4 μM NPA inhibits lateral root reorientation in both upward (A) and

737 downward (B) directions. n = 25-37 roots for each treatment from 3 biologically

738 independent experiments. One-way ANOVA followed by post-hoc Tukey's HSD test

739 revealed F (5) = 13.7890 for (A) and 25.8968 for (B) gave p values = $1.102X10^{-16}$ for (A)

740 and (B). (C) Change in length of stage III lateral roots during mock and NPA treatments.
741 The growth rates of NPA treated roots are not significantly different from mock treated
742 roots (p = 0.0838) n = 10 roots per treatment from 3 biologically independent
743 experiments. (D) Visualization of auxin fluxes using the auxin reporter DII-Venus in
744 upward and downward reoriented lateral roots. Scale bar = 20 μm (D,E) Ratio of mean
745 nuclear fluorescence between upper and lower epidermal cells of Stage III lateral roots
746 gravistimulated 30º above or below their GSA using the auxin reporter DII-Venus. Note: to
747 aid understanding, the colloquial terms up- and down-bending are used as short
748 descriptors of lateral roots undergoing negative (upward) and positive (downward)
749 gravitropic response respectively. *n* = 10-15 roots analysed for each angle. Roots were
750 reoriented from their GSA on the rotating stage of a vertical confocal microscope and
751 imaged 60 mins post reorientation. One-way ANOVA followed by post-hoc Tukey's HSD
752 test revealed F (2) = 6.325 gave p value of 0.0039 (F,G) Quantification of atrichoblast
753 epidermal cell lengths at upper and lower sides of reorientated lateral roots. In upward
754 bending lateral roots, epidermal cells on the bottom half of the root are significantly longer
755 than those on the upper side (F middle panel, G). In contrast, in downward bending
756 lateral roots, epidermal cells on the bottom of the root are significantly shorter in length
757 than those on the upper side (F third panel, G). Scale bar = 50 μm. n= 20-35 for each
758 group from 3 biologically independent experiments. One-way ANOVA followed by post-
759 hoc Tukey's HSD test revealed F (5) = 13.7890 gave p value of $5.2996 \times 10^{-11}$ (H) Kinetics
760 of gravitropism in lateral roots growing at oblique orientations. Curvature was measured
761 in terms of stage rotation for roots maintained 30° from their original orientation by a
762 feedback system following either an upward reorientation, resulting in positive
763 gravitropism, or a downward reorientation, resulting in negative gravitropism (mean ± SE,
764 *n* = 18 – 22). (I) Ratio of mean nuclear DII-Venus fluorescence between upper and lower
765 epidermal cells of Stage III lateral roots gravistimulated above or below their GSA by

766 different angles. Roots were gravistimulated for 90 mins prior to imaging. *n* =8-10 roots
767 for each angle of stimulation from 3 biologically independent experiments.

768 **Figure 2: PIN polarity distribution in lateral roots**

769 (A,B) Comparison of PIN polarity in lateral roots at their GSA and primary roots reoriented
770 by 45º roots in seedlings expressing PIN3:GFP (A) and PIN7:GFP (B). Fluorescence was
771 measured on upper and lower membranes of outer columella cells as indicated in Fig.
772 S1C. PIN3 shows a slight polarity towards the lower cell membrane (A), while, In contrast,
773 PIN7:GFP shows enhanced polarity towards the upper membrane (B) in lateral roots
774 growing at their GSA. However, both PIN3:GFP (A ) and PIN7:GFP (B) are predominantly
775 polarized towards the lower plasma membrane in primary roots reoriented by ~45° for 30
776 mins (C). Scale bar = 15 μm (A,B) n = 20-25 roots from 3 biologically independent
777 experiments. Statistical analysis was carried out using a pairwise two-tailed T-test.
778 Comparison of reorientation kinetics in lateral roots of 12-day-old WT Col-0 (D), *pin3 pin7*
779 (E), *pin3pin4pin7* (F), *pin3pin4* (G), *pin3-3* (H) and *pin7-2* (I) seedlings gravistimulated
780 both above and below their GSA. BR represents GSA before reorientation. Average GSA
781 of 10-12 upward and downward bending stage III lateral roots was quantified after
782 reorientation until the roots were within 5 degrees of their original GSA. Black asterisks
783 indicate the time point at which angles were recovered for downward bending roots, while
784 magenta asterisks indicate the time point at which angles were recovered for upward
785 bending roots. *pin3* land *pin3pin4* lateral roots reorientate upwards significantly faster (G,
786 H), while *pin7* lateral roots reorientate downwards at a faster rate (I). WT Col-0 control
787 lateral roots reorientate back to their GSA in both directions in approximately 6 hours (D).
788 In contrast, reorientation in both directions is delayed in the *pin3 pin7* double mutant (E)
789 and is virtually negligible in the *pin3pin4pin7* triple mutant (F). n = 15-21 roots at all time
790 points (D-I) from 3 biologically independent experiments. Bars represent standard error of
791 the means.

792 **Figure 3: PIN phosphorylation affects PIN polarity and redistribution kinetics in**
793 **lateral root statocytes**

794 (A-D) PIN polarity distribution in columella cells of lateral roots rotated around their axis of
795 growth by 45º ('flip assays', see Figure S3A for a diagrammatic description of the
796 experiment). In all panels, the former upper side of the columella cell is towards the top of
797 the page. Post flip, phosphorylated PIN3 and PIN7 are retained on the upper plasma
798 membrane for approximately 30 mins longer than lower side unphosphorylated PINs.
799 PIN3 (A,B) and PIN7 (C,D) polarity gradually becomes symmetrical on upper and lower
800 sides of the plasma membrane 2 hours after 'flipping' (D). Scale bar = 5 μm. n = 25-31
801 roots for each time point for (B) and (D) from 3 biologically independent experiments. One
802 way ANOVA followed by post-hoc Tukey's HSD test revealed F stat (3) = 3.8028 with a p
803 value of 0.01027 for B and 5.8904 with a p value of 0.01456 for D. (E,F) Quantification of
804 PIN3 polarity in transgenic lines expressing nonphosphorylatable (S>A) or phosphomimic
805 (S>D) variant of PIN3-YFP. Scale bar = 15 μm. n = 21 roots for each line from 3
806 biologically independent experiments. One way ANOVA followed by post-hoc Tukey's
807 HSD test revealed F stat (2) = 10.692 with a p value of 0.0001. (G,H) PIN3::YFP polarity
808 ratios after 30 mins in horizontally flipped lateral roots in transgenic PIN3 phosphovariant
809 lines. PIN3::YFP polarized to the upper side 30 mins after flipping in WT PIN3 and PIN3
810 S>D: YFP phosphomimic lines, but not in the PIN3 S>A:YFP phosphodead line. Scale
811 bar = 10 μm. n = 21 roots for each line from 3 biologically independent experiments. One
812 way ANOVA followed by post-hoc Tukey's HSD test revealed F stat (2) = 4.541 with a p
813 value of 0.0498. (I,J) Quantification of lateral root GSA phenotypes in *rcn1* and *wag1*
814 *wag2* mutants. *rcn1* lateral roots have significantly less vertical lateral roots as compared
815 to WT Ws seedlings (I). In contrast, *wag1 wag2* seedlings have significantly more vertical
816 lateral roots than WT Col-0 controls (J). n = 21 roots for each genotype from 3 biologically
817 independent experiments (I,J). Statistical analysis was performed using two tailed T-tests
818 (I,J).

819 **Figure 4: Auxin regulates lateral root GSA through an RCN1-dependent PIN3**
820 **module**

821 (A,B) Overexpression of *RCN1* driven by the *ARL2* promoter (ARL2::RCN1) in a WT Col-
822 0 background results in a significantly more vertical lateral root GSA phenotype in
823 contrast to Col-0 control (A) and restores the GSA of *rcn1* lateral roots (B). n = 15-25 for
824 each genotype from 3 biologically independent experiments for both (A) and (B).
825 Statistical analysis was performed using a two tailed T-test for (A) and a one way ANOVA
826 with an F stat (2) = 19.3276 with a p value = $4.188 \times 10^{-5.}$ (C,D) RCN1:GFP protein levels
827 in ten day old lateral roots treated with 50 nM IAA for 4 hours. Auxin treatment results in a
828 significant increase in GFP signal in the columella cells of RCN1:GFP lateral roots. n =
829 15-21 roots per treatment from 3 biologically independent experiments. Statistical
830 analysis was performed using a two tailed T-test (D). Red dashed lines represent
831 columella area used for quantification in (C). Scale bar = 20 μm in (C). (E,F)
832 Overexpression of *RCN1* in lateral root columella cells leads to a significant shift in
833 PIN3:GFP polarity towards the lower side of the cell. In contrast, PIN7:GFP polarity is
834 unaffected. n = 18-24 for each genotype from 3 biologically independent experiments.
835 Statistical analysis was performed using a pairwise two tailed T-test. Scale bar = 15 μm
836 (E). (G). The PP2A/RCN1 subunit is able to dephosphorylate the central hydrophilic loop
837 of PIN3 *in vitro.* The experiment was repeated independently three times with similar
838 results.

839 **Figure 5: Model of auxin-dependent regulation of GSA**

840 (A) Model of GSA control in the lateral root in which phosphorylated PIN3 & PIN7 mediate
841 upward, antigravitropic auxin flux from columella cells, while unphosphorylated PIN3 &
842 PIN7 mediate downward, gravitropic auxin transport. In addition to regulating cell
843 elongation further back along the root, auxin also positively regulates levels of the PIN
844 phosphatase subunit RCN1, thereby diminishing the magnitude of AGO. This causes the
845 equilibrium between angle-dependent gravitropic- and angle-independent antigravitropic
846 auxin flux to occur at a more vertical setpoint angle. (B) Tropic response to displacement
847 either above or below GSA is driven by angle-dependent changes in downward

gravitropic auxin flux acting in tension with a more constant, angle-independent upward antigravitropic auxin flux. The thickness of red and green arrows signify relative auxin flux.

**References**


1. Digby, R.D. & Firn, J. The gravitropic set-point angle (GSA): the identification of an important developmentally controlled variable governing plant architecture. *Plant Cell Environ*. **18**, 1434-40 (1995).
2. Nemec, B. Ueber die art der wahrnehmung des schwek- raftreizes bei den pflanzen. *Ber Dtsch Bot Ges* **18,** 241–245 (1900).
3. Haberlandt, G. Ueber die perzeption des geotropischen reizes. *Ber Dtsch Bot Ges* **18,** 261–272 (1900).
4. Sack, F.D. & Kiss, J.Z. Rootcap structure in wild-type and in a starchless mutant of Arabidopsis. *Am. J. Bot*. **76**, 454-64 (1989).
5. Cholodny, N. Wuchshormone und tropismem bei den pflanzen. Biologosches Zentralblatt, **47**, 604-626 (1927).
6. Went FW. Wuchsstoff und Wachstum. *Extrait du Recueil des Travaux Botaniques Neerlandais*; **25**:1–116 (1928).
7. Friml, J., Wisniewska, J., Benková, E., Mendgen, K. & Palme, K. Lateral relocation of auxin efflux regulator AtPIN3 mediates tropism in Arabidopsis. *Nature*, **415**, 806-9 (2002).
8. Luschnig, C., Gaxiola, R. A., Grisafi, P., & Fink, G. R. EIR1, a root-specific protein involved in auxin transport, is required for gravitropism in Arabidopsis thaliana. *Genes & devel*, ***12***, 2175–2187. https://doi.org/10.1101/gad.12.14.2175. (1998).

876 9. Blancaflor, E. & Masson, P. Plant Gravitropism. Unravelling the ups and downs of
877 a complex process. *Plant Physiol.* **133**, 1677-90 (2003).
878 10. Kleine-Vehn, J., Ding, Z., Jones, A.R., Tasaka, M., Morita, M.T. & Friml, J. Gravity-
879 induced PIN transcytosis for polarization of auxin fluxes in gravity-sensing root
880 cells. *Proc Natl Acad Sci*. USA **107**, 22344-22349 (2010).
881 11. Rakusova, H., Gallego-Bartoleme, J., Vanstraelen, M., Boisivon, H., Alabadi, D.,
882 Blazquez, M.A., Benkova, E., Friml, J. Polarisation of PIN3-dependent auxin
883 transport for hypocotyl gravitropic response in *Arabidopsis thaliana*. *Plant J.* **67**,
884 817-826 (2011).
885 12. Sukumar, P., Edwards, K. F., Rahman, K., DeLong, A. & Muday, G.K. PINOID
886 Kinase Regulates Root Gravitropism through Modulation of PIN2-Dependent
887 Basipetal Auxin Transport in Arabidopsis. Plant Physiol. 150, 722-735 (2009).
888 13. Rehman, A., Takahashi, M., Shibasaki, K., Wu, S., Inaba, T., Tsurumi, S. &
889 Baskin, T. Gravitropism of Arabidopsis thaliana roots requires the polarization of
890 PIN2 toward the root tip in meristematic cortical cells**.** *Plant Cell* **22**, 1762-76
891 (2010).
892 14. Glanc M., Fendrych M. & Friml J. Mechanistic framework for cell-intrinsic re-
893 establishment of PIN2 polarity after cell division. *Nature Plants* **4**, 1082-1092
894 (2018).
895 15. Mullen, J.P. & Hangarter, R. Genetic analysis of the gravitropic set-point angle in
896 lateral roots of Arabidopsis. *Adv. Space Res.* **31**, 2229-22364 (2003).
897 16. Roychoudhry, S., Del Bianco M., Kieffer, M. & Kepinski, S. Auxin controls
898 gravitropic setpoint angle in higher plant lateral organs. *Curr. Biol.* **23**, 1497-1504
899 (2013).
900 17. Roychoudhry, S. & Kepinski, S. Root and shoot branch growth angle control – The
901 wonderfulness of lateralness. *Curr. Op. Plant Biol.* **23,**124-131 (2015a).

902 18. Ruiz Rosquete, M., von Wangenheim, D., Marhavy, P., Barbez, E., Stelzer,
903 E.H.K., Benkova, E., Maizel, A. & Kleine-Vehn, J. An auxin transport mechanism
904 restricts positive orthogravitropism in lateral roots. *Curr. Biol.* **23**, 817-822 (2013).
905 19. Ruiz Rosquete M., Waidmann S. & Kleine-Vehn J. PIN7 auxin carrier has a
906 preferential role in terminating radial root expansion in Arabidopsis thaliana*. Int J.*
907 *Mol. Sci*. **19**, 1238 – 1242 (2018).
908 20. Guyomarc'h, S., Leran, S., Auzon-Carpe, M., Perrine-Walker, F., Lucas, M. &
909 Laplaze, L. Early development and gravitropic response of lateral roots in
910 *Arabidopsis thaliana*. *Phil. Trans. R. Soc. Lond. B. Biol. Sci.* **367**, 1509-1516
911 (2012).
912 21. Kiss, J.Z., Miller K.M., Ogden L.A. & Roth K.K. Phototropism and gravitropism in
913 lateral roots of Arabidopsis. *Plant Cell Physiol.* **43**, 35-43 (2002).
914 22. Ogura T., Goeschl C., Filiault D., Mirea M., Slovak R., Wohlrab B., Satbhai S.B. &
915 Busch W. Root system depth in Arabidopsis is shaped by EXOCYST70A3 via the
916 dynamic modulation of auxin transport. *Cell* **178,** 400 – 412 (2019).
917 23. Abas L, Kolb M, Stadlmann J, *et a*l. Naphthylphthalamic acid associates with and
918 inhibits PIN auxin transporters [published correction appears in Proc Natl Acad Sci
919 U S A. 2021 Mar 9;118(10):]. *Proc Natl Acad Sci U S A*;**118**:e2020857118 (2021).
920 24. Band, L.R., Wells, D.M., Larrieu, A., Sun, J., Middleton, A. M., French, A. P., *et al*.
921 Root gravitropism is regulated by a transient lateral auxin gradient controlled by a
922 tipping-point mechanism. *Proc. Natl. Acad. Sci.* USA **109**, 4668-73 (2012).
923 25. Liao, C.Y., Smet, W., Brunoud, G., Yoshida, S., Vernoux, T. & Weijers, D.
924 Reporters for sensitive and quantitative measurement of auxin response. *Nat.*
925 *Methods* **12,** 207-210 (2015).
926 *26.* Roychoudhry, S., Kieffer, M., Del Bianco, M., Liao, C.Y., Weijers, D. & Kepinski, S.
927 The developmental and environmental regulation of gravitropic setpoint angle in
928 Arabidopsis and bean. *Sci. Rep.* **7,** 42664 | *DOI: 10.1038/srep42664* (2017)

929 27. Fendrych, M., Akhmanova, M., Merrin, J., Glanc, M., Hagihara, S., Takahashi, K.,
930 Uchida, N., Torii, K.U. & Friml, J. Rapid and Reversible Root Growth Inhibition by
931 TIR1 Auxin Signalling. Nat. Plants 2018, 4, 453–459 (2018).
932 28. Mullen, J., Wolverton, C., Ishikawa, H. & Evans, M.L. Kinetics of Constant
933 Gravitropic Stimulus Responses in Arabidopsis Roots Using a Feedback System.
934 *Plant Physiol.* **23**, 665–670 (2000).
935 29. von Wangenheim, D., Hauschild, R., Fendrych, M., Barone, V., Benkova, E. &
936 Friml J. Live tracking of moving samples in confocal microscopy for vertically
937 grown roots. *eLife* **6**, e26792 (2017).
938 30. Vieten, A., Vanneste, S., Wisniewska, J., Benkova, E., Benjamins, R., Beeckman,
939 T., Luschnig, C. & Friml, J. Functional redundancy of PIN proteins is accompanied
940 by auxin- dependent cross-regulation of PIN expression. *Development* **132**, 4521-
941 4531 (2006).
942 *31.* Zadnikova P., Petrasek J., Marhavy P.,Raz V., Vandenbussche F., Ding
943 Z.,Schwarzerova K., Morita M.T., Tasaka M., Hejatko J., Van Der Straeten D.,
944 Friml J. & Benkova E. Role of PIN-mediated auxin efflux in apical hook
945 development of *Arabidopsis thaliana. Devel.* ***137****, 607-617* (2010).
946 32. Friml J., Vieten, A., Sauer, M., Weijers, D., Schwarz, H., Hamann, T., Offringa, R.
947 & Jürgens, G. Efflux-ependent auxin gradients establish the apical–basal axis of
948 Arabidopsis. *Nature* **426**, 147–153 (2003)
949 33. Zhang, J., Nodzyński, T., Pěnčík, A., Rolčík, J. & Friml, J. PIN phosphorylation is
950 sufficient to mediate pin polarity and direct auxin transport. *Proc Natl Acad Sci*.
951 USA **107**, 918-922 (2009).
952 34. Adamowski, M. & Friml, J. PIN-dependent auxin transport: action, regulation, and
953 evolution *Plant Cell* **27**, 20-32 (2015).
954 35. Geldner, N., Denervaud-Tendon, V., Hyman, D.L., Mayer, U., Stierhof, Y.D. &
955 Chory, J. Rapid, combinatorial analysis of membrane compartments in intact
956 plants with a multicolor marker set. *Plant J.* **59**, 169–178 (2009).

957 36. Dhonukshe, P., Huang, F., Galvan-Ampudia, C. S., Mahonen, A. P., Kleine-Vehn,
958 J., Xu, J., Quint, A., Prasad, K., Friml, J., Scheres, B. & Offringa R. Plasma
959 membrane-bound AGC3 kinases phosphorylate PIN auxin carriers at TPRXS(N/S)
960 motifs to direct apical PIN recycling. *Development* **137**, 3245-55 (2010).
961 37. Friml, J., Yang, X., Michniewicz, M., Weijers, D., Quint, A., Tietz, O., Benjamins,
962 R., Ouwerkerk, P. B.F., Ljung, K., Sandberg, S., Hooykaas, P.J.J., Palme, K. &
963 Offringa, R. (2004). A PINOID-dependent binary switch in apical-basal polar PIN
964 targeting directs auxin efflux. *Science* **306**, 862-865.
965 38. Michniewicz, M., Zago, M. K., Abas, L., Weijers, D., Schweighofer, A., Meskiene,
966 I., Heisler, M. G., Ohno, C., Zhang, J., Huang, F., Schwab, R., Weigel, D.,
967 Meyerowitz, E. M., Luschnig C., Offringa R. & Friml, J. Antagonistic regulation of
968 PIN phosphorylation by PP2A and PINOID directs auxin flux. *Cell* **130**, 1044–1056
969 (2007).
970 39. Grones P., Abas M., Hajny J., Jones A., Weidmann S., Kleine-Vehn J. & Friml J.
971 PID/WAG-mediated phosphorylation of the Arabidopsis PIN3 auxin transporter
972 mediates polarity switches during gravitropism. *Sci. Rep* **8**, 10279 (2018).
973 40. Zourelidou, M., Absmanner, B., Weller, B., Barbosa, I. C., Willige, B. C., Fastner,
974 A., Streit, V., Port, S. A., Colcombet, J., de la Fuente van Bentem, S., Hirt, H.,
975 Kuster, B., Schulze, W. X., Hammes, U. Z. & Schwechheimer, C. (2014). Auxin
976 efflux by PIN-FORMED proteins is activated by two different protein kinases, D6
977 PROTEIN KINASE and PINOID. *eLife* ***3*** e02860
978 41. Harrison, B.R. & Masson, P.H. ARL2, ARG1 and PIN3 define a gravity signal
979 transduction pathway in root statocytes. *Plant J.* **53**, 380–392 (2008).
980 42. Robert, S., Kleine-Vehn J., Barbez E., Sauer M., Paciorek T., Baster P., Vanneste
981 S., Zhang J., Simon, S., Covanova, M., Hayashi, K., Dhonukshe P., Yang Z.,
982 Bednarek S.B., Jones A.M., Luschnig C., Aniento F., Zazimalova E. & Friml J.
983 ABP1 Mediates Auxin Inhibition of Clathrin-Dependent Endocytosis
984 in Arabidopsis. *Cell* **143**, 111 – 121 (2010).

43. Perbal, G., & Driss-Ecole, D. Microgravite et gravitropisme racinaire [Microgravity and root gravitropism]. *Acta botanica Gallica : bulletin de la Societe botanique de France*, **140,** 615–632 (1993).
44. Sack F. D. Plant gravity sensing. *International review of cytology*, **127**, 193–252 (1991).
45. Galván-Ampudia, C. S., & Offringa, R. Plant evolution: AGC kinases tell the auxin tale. *Trends in pl. sci.*, **12**, 541–547 (2007).
46. Ganguly, A., Sasayama, D. & Cho H.-T. Regulation of the polarity of protein trafficking by phosphorylation. *Mol. Cells* **33,** 423–30 (2012).
47. Waidmann, S., Ruiz Rosquete, M., Schöller, M., Sarkel, E., Lindner, H., LaRue, T., Petřík, I., Dünser, K., Martopawiro, S., Sasidharan, R., Novak, O., Wabnik, K., Dinneny, J. R., & Kleine-Vehn, J. Cytokinin functions as an asymmetric and anti-gravitropic signal in lateral roots. *Nat. comm.*, *10*(1), 3540. (2019).
48. Ge, L. & Chen, R. Negative gravitropism in plant roots. *Nature Plants* **2**, 16155-59 (2016).
49. Guseman, J.M., Webb, K., Srinivasan, C. & Dardick, C. DRO1 influences root system architecture in Arabidopsis and *Prunus* species. *Plant J.* **89**, 1093–1105 (2017).
50. Taniguchi, M., Furutani, M., Nishimura, T., Nakamura, M., Fushita, T., Iijima, K., Baba, K., Tanaka, H., Toyota, M., Tasaka, M. & Morita, M.T. The Arabidopsis LAZY1 family plays a key role in gravity signaling within statocytes and in branch angle control of roots and shoots. *Plant Cell* **29**, 1984-1999 (2017)
51. Yoshihara, T. & Spalding, E.P. LAZY Genes Mediate the Effects of Gravity on Auxin Gradients and Plant Architecture. *Plant Physiol.* **175**, 959-969 (2017).
52. Furutani, M., Hirano, Y., Nishimura, T. *et al.* Polar recruitment of RLD by LAZY1-like protein during gravity signaling in root branch angle control. *Nat Commun.* **11,** 76-89 (2020).

53. Rashotte, A. R., Brady, S. R., Reed, R. C., Ante, S. J. & Muday, G. K. Basipetal auxin transport is required for gravitropism in roots of Arabidopsis. *Plant Physiol.* **122**, 481-490 (2000).

54. Santner, A.A. & Watson, J.C. The WAG1 and WAG2 protein kinases negatively regulate root waving in Arabidopsis. *Plant J.* **45**, 752-764 (2006).

55. Roychoudhry, S & Kepinski, S (2023). Antigravitropic PIN polarization maintains non-vertical growth in lateral roots (Version 1). Zenodo. https://doi.org/10.5281/zenodo.8019902

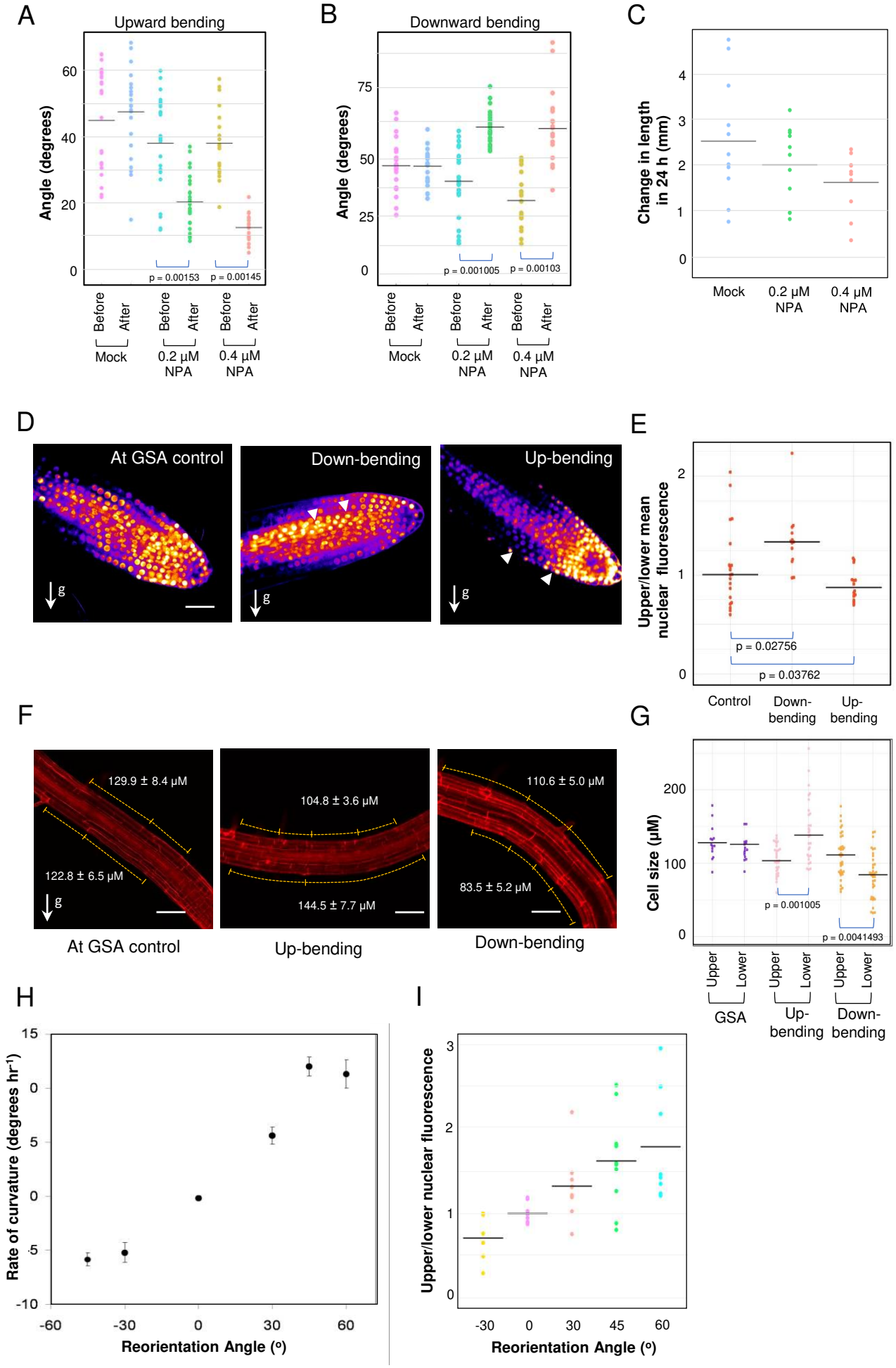
A
Upward bending
Angle (degrees)
p = 0.00153
p = 0.00145
Before
After
Mock
0.2 μM NPA
0.4 μM NPA
B
Downward bending
Angle (degrees)
p = 0.001005
p = 0.00103
C
Change in length in 24 h (mm)
D
At GSA control
Down-bending
Up-bending
g
E
Upper/lower mean nuclear fluorescence
p = 0.02756
p = 0.03762
Control
Down-bending
Up-bending
F
129.9 ± 8.4 μM
122.8 ± 6.5 μM
104.8 ± 3.6 μM
144.5 ± 7.7 μM
110.6 ± 5.0 μM
83.5 ± 5.2 μM
At GSA control
Up-bending
Down-bending
G
Cell size (μM)
p = 0.001005
p = 0.0041493
Upper
Lower
GSA
Up-bending
Down-bending
H
Rate of curvature (degrees hr⁻¹)
Reorientation Angle (°)
I
Upper/lower nuclear fluorescence
Reorientation Angle (°)

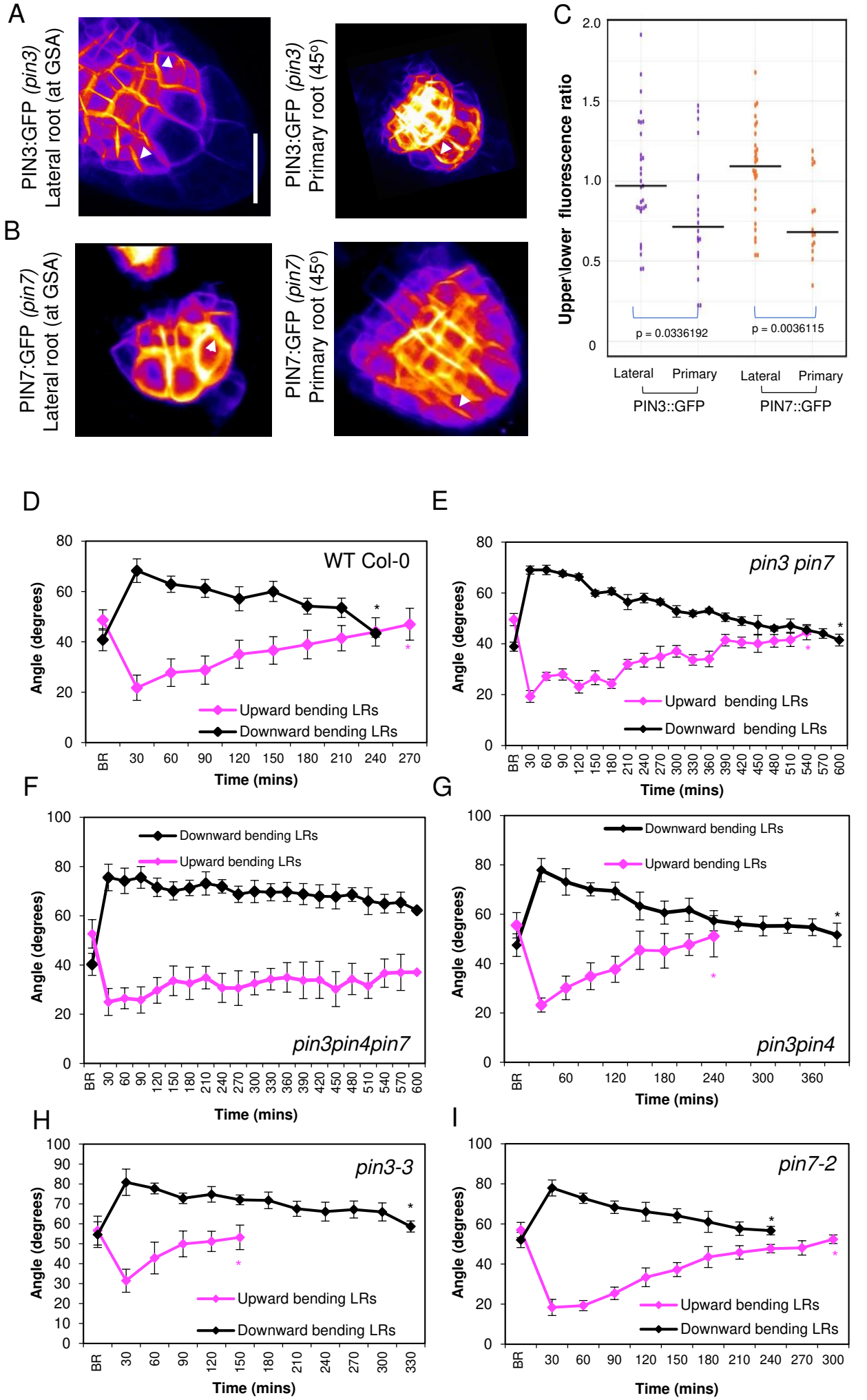


Roychoudhry et al. Figure 2

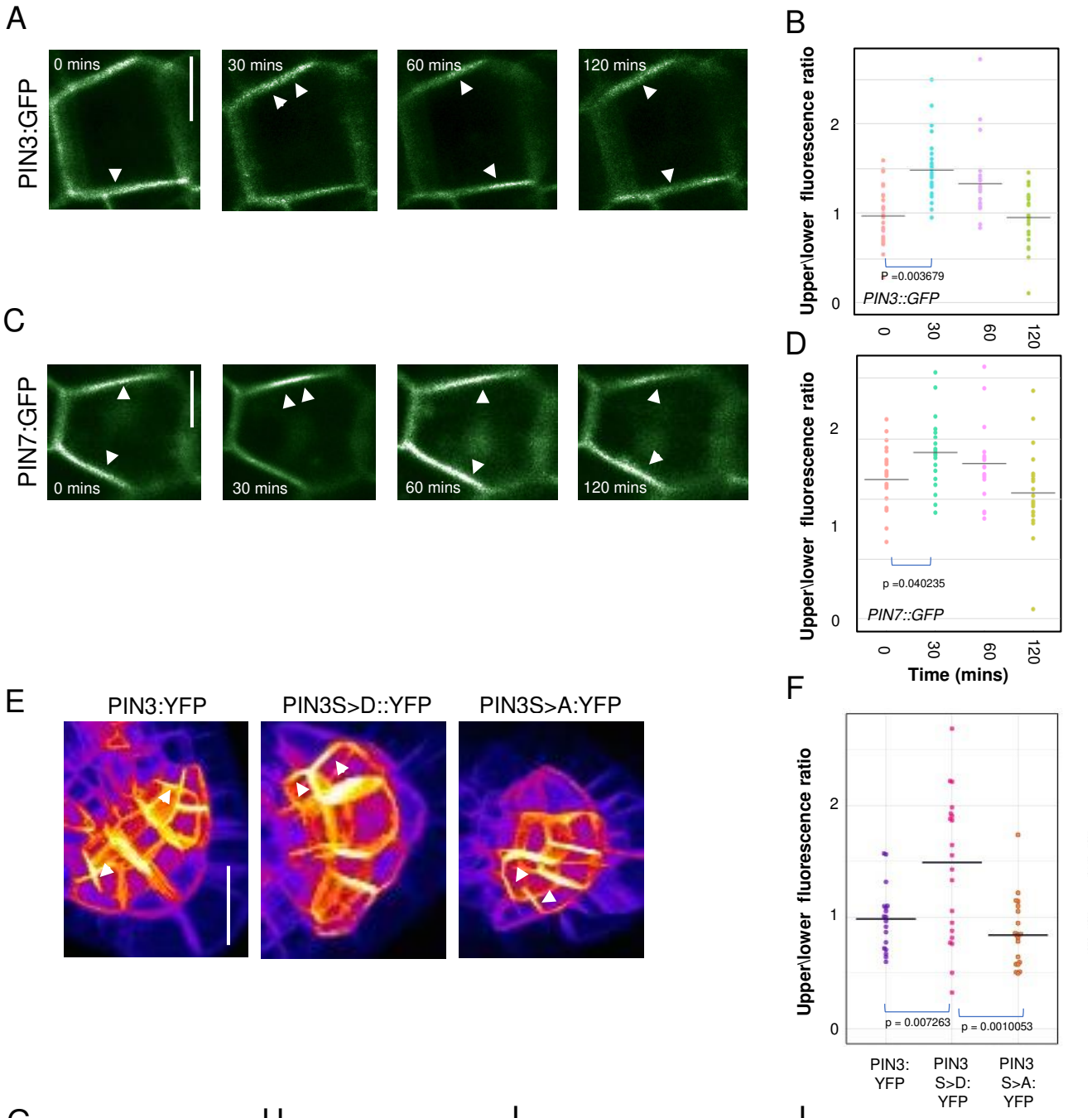


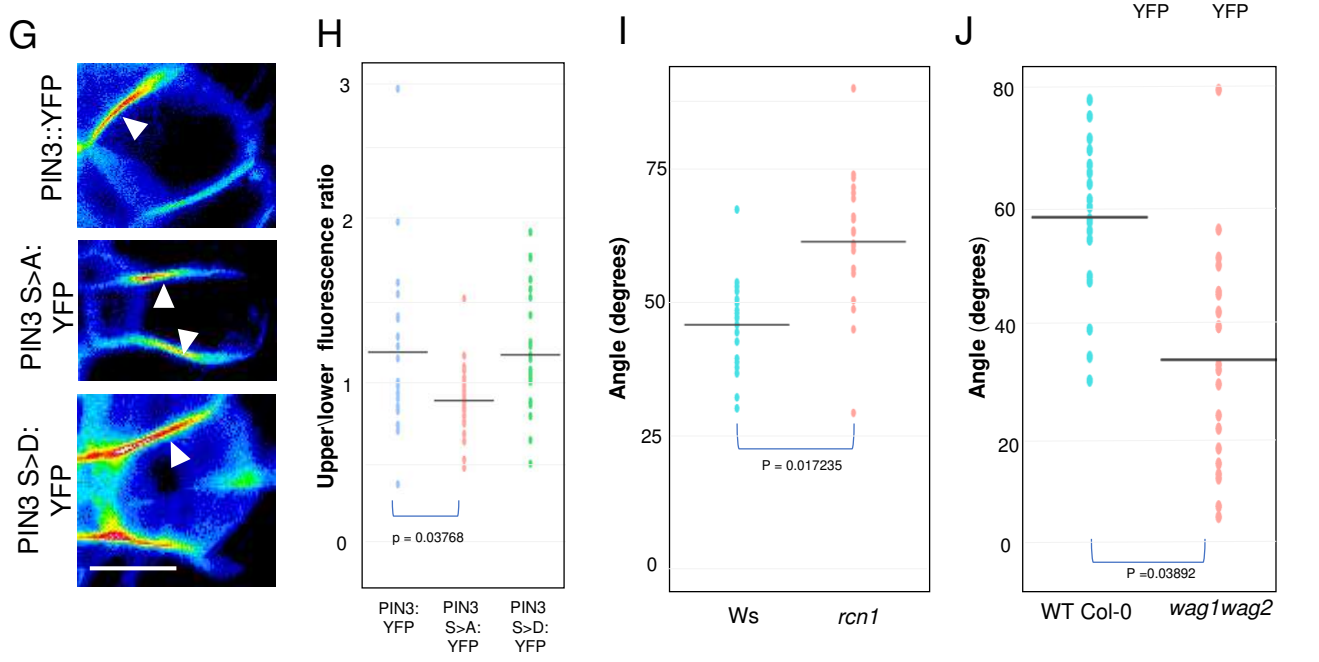


Roychoudhry et al. Figure 3

Roychoudhry et al. Figure 4

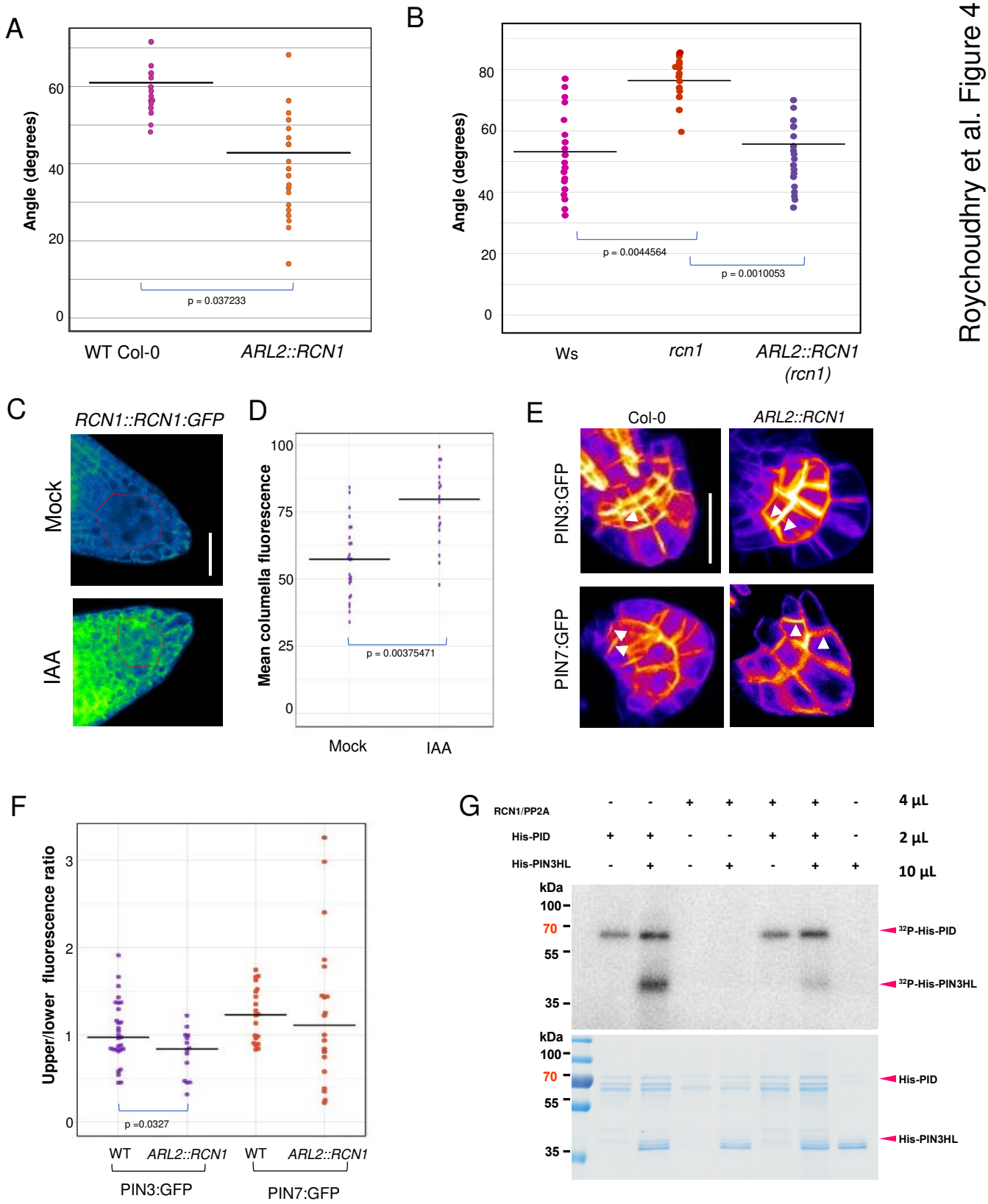

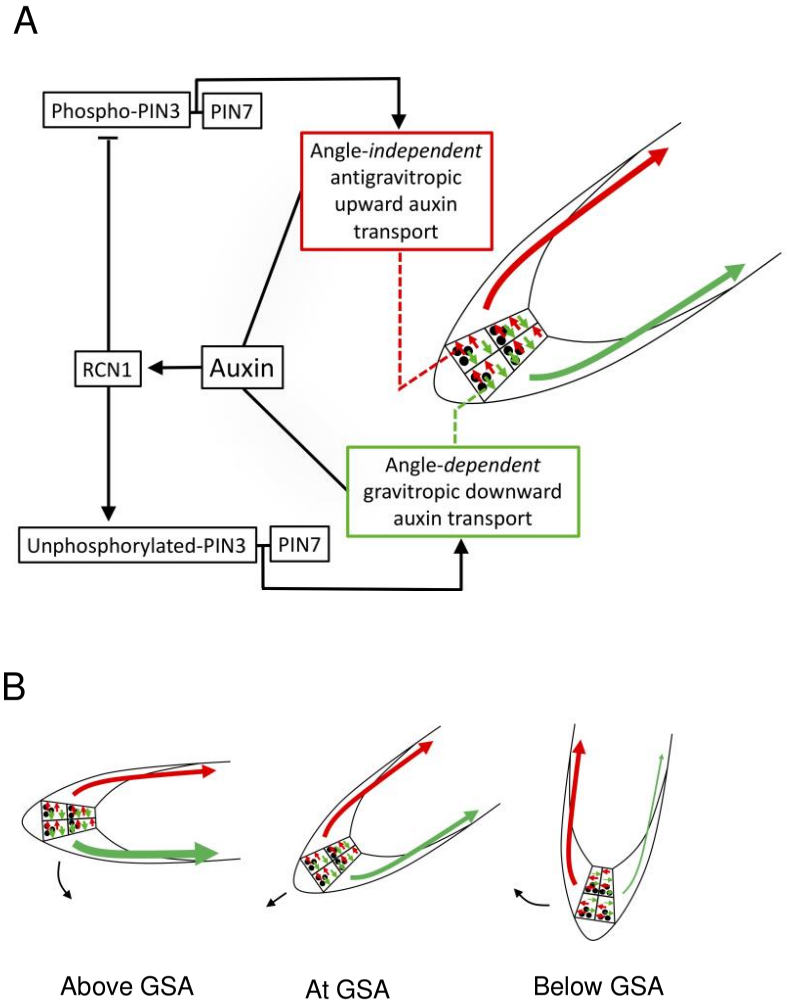
A
Phospho-PIN3
PIN7
Angle-*independent* antigravitropic upward auxin transport
RCN1
Auxin
Angle-*dependent* gravitropic downward auxin transport
Unphosphorylated-PIN3
PIN7
B
Above GSA
At GSA
Below GSA

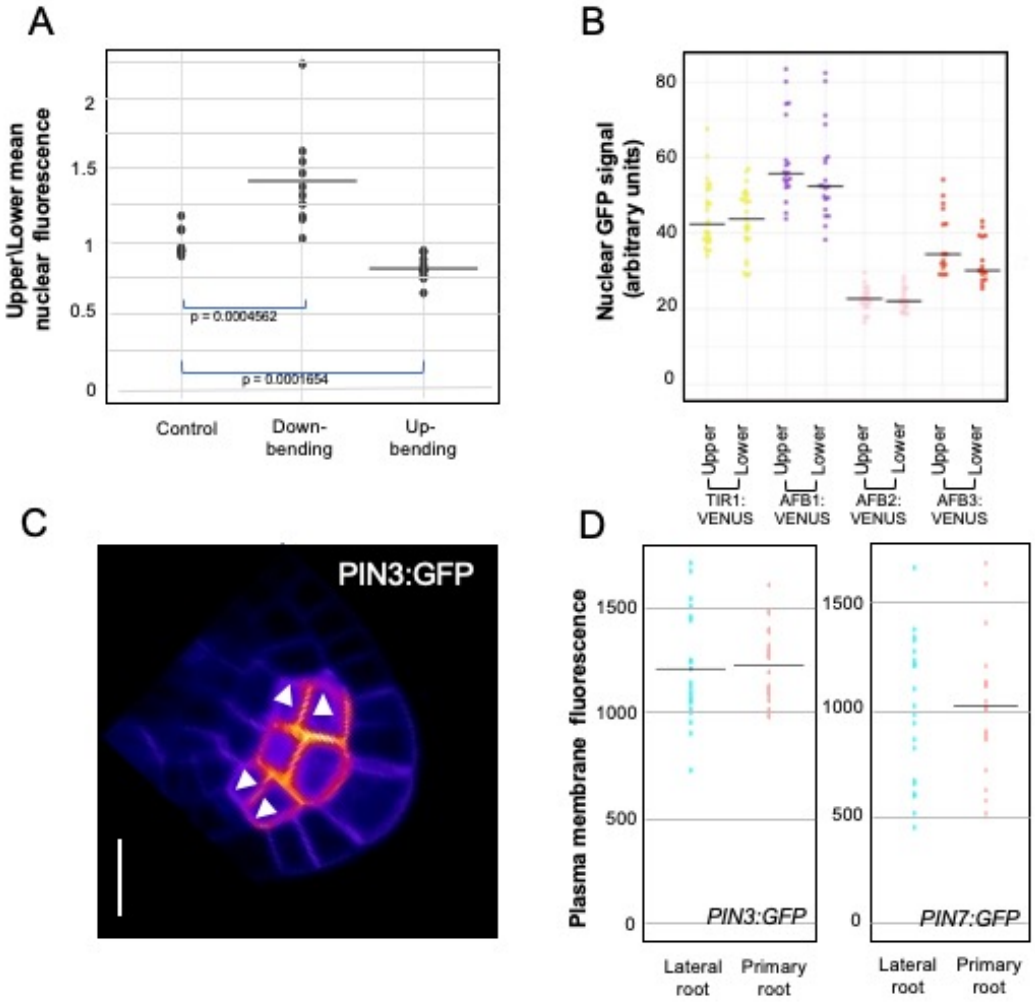


**Figure S1**: (A) Ratio of nuclear R2DII signal across upper and lower epidermal cells in lateral roots at GSA (control) and reorientated upwards and downwards. Images were taken 90 mins post reorientation Bars represent standard error of mean nuclear fluorescence. n = 12-15 roots for each orientation from 3 biologically independent experiments. One way ANOVA revealed F stat (2) = 22.25654 with a p value = 0.001346. (B) Statistical analysis using pairwise two-tailed T tests revealed no significant difference in mean nuclear fluorescence of TIR1/AFB:Venus in atrichoblast cells on the upper and lower side of stage III lateral roots. n = 39-51 nuclei analysed for each transgenic line across 3 biologically independent experiments. (C) Outer membranes (white arrowheads) of upper and lower cells of the central columella used for quantification of PIN polarity in a single stack of a PIN3:GFP lateral root. Scale bar = 5 μm. (D) Quantification of PIN3/7::GFP fluorescence levels in plasma membranes of columella cells from stage III lateral and primary roots. n = 21-25 roots for each transgenic line quantified from 3 biologically independent experiments. Pairwise two tailed T-tests revealed no significant differences in membrane fluorescence levels.

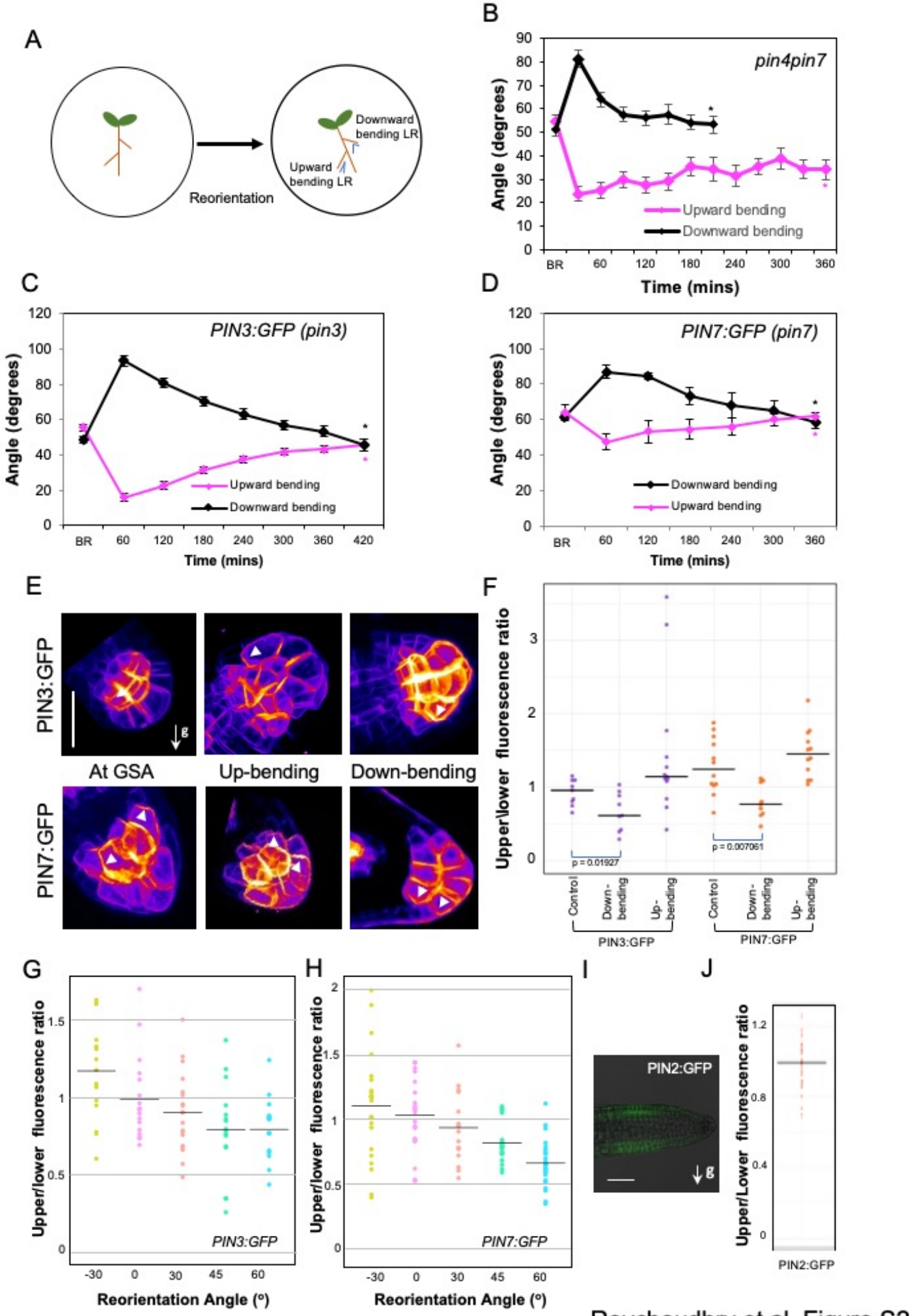


Roychoudhry et al. Figure S2

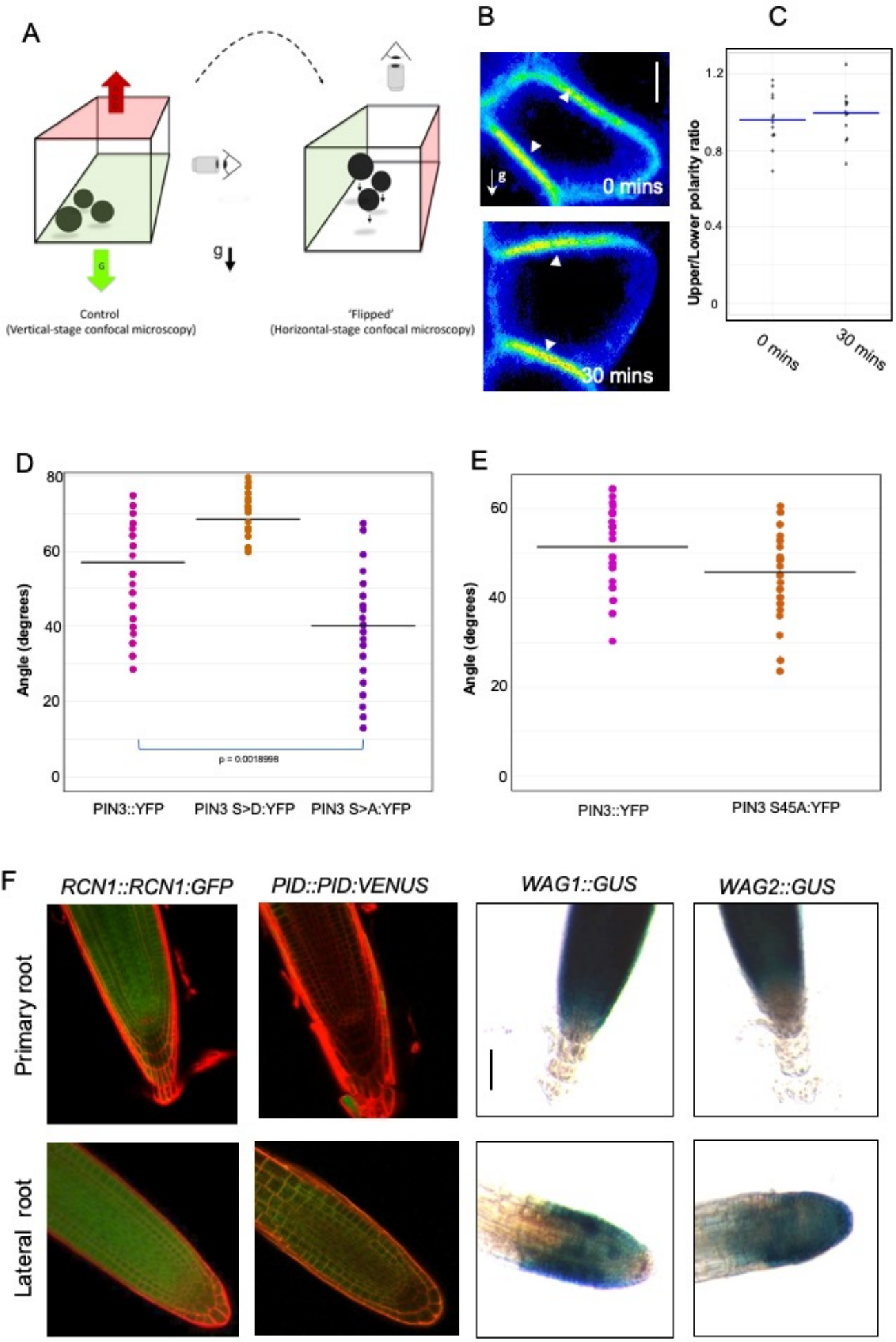


Roychoudhry et al. Supp. Fig. S3

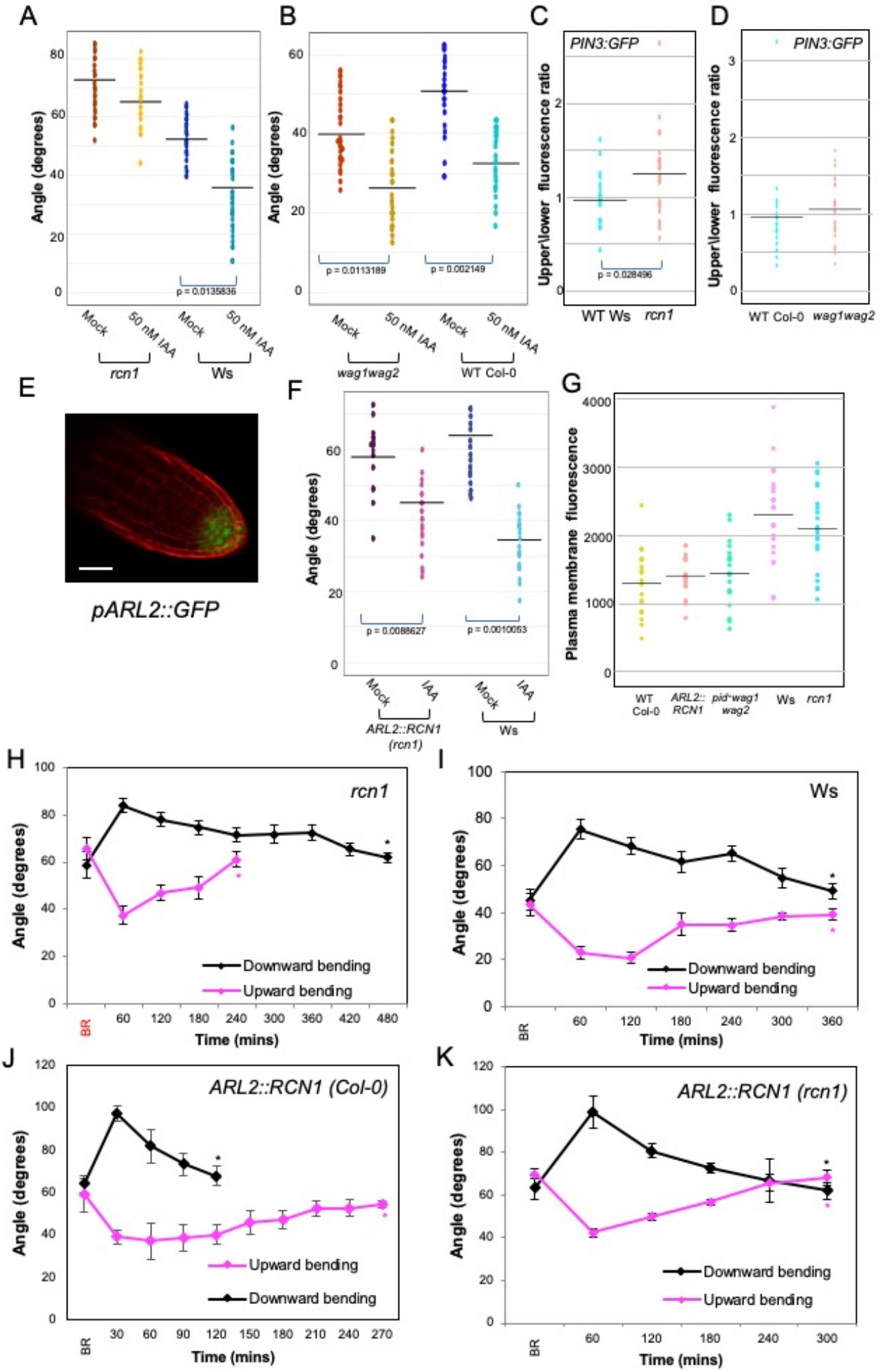


Roychoudhry et al. Supp. Fig. S4

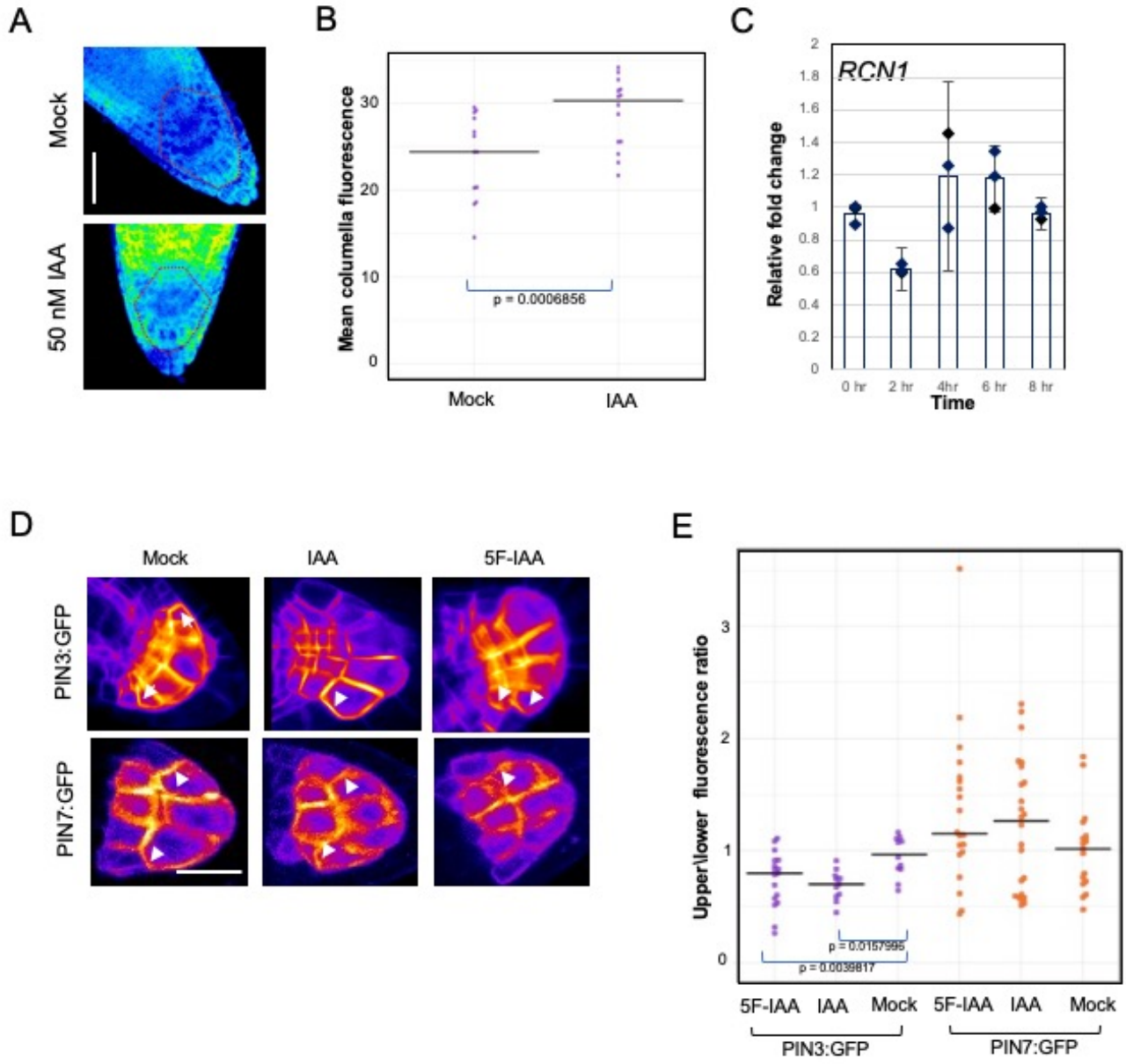


**Figure S5** (A,B) Effect of auxin treatment for 4 hours on *RCN1::RCN1:GFP* (*PP2AA::PP2AA:GFP* translational reporter line) primary root columella cells. Auxin treatment leads to a significant increase in RCN1:GFP signal levels. n = 15-21 roots from 3 biologically independent experiments. Statistical analysis was performed using a two tailed T-test. Scale bar = 20 µm. Red dashed lines represent area of columella signal quantification in (A). (C) Effect of 50 nM IAA on *RCN1* transcript levels in lateral root columella cells. No significant increase in *RCN1* levels occurred over an 8 hour time course. Data represent averages from 3 independent experiments with 7-8 root tips harvested for each time point per experiment. Bars represent standard error of the means. (D,E) Treatment with 50 nM IAA or 5F-IAA results in a shift in PIN3:GFP polarity towards the lower side of the columella cell, but has no effect on PIN7:GFP polarity. n = 12-15 roots per treatment from 3 biologically independent experiments. One way ANOVA revealed an F stat(5) value = 4.9116 with a p value = 0.0130.